Centrifuge modelling of the influence of slope height on the seismic performance of rooted slopes

Liang, T.; Knappett, J. A.

Published in:
Géotechnique

DOI:
10.1680/jgeot.16.P.072

Publication date:
2017

Licence:
Other

Document Version
Peer reviewed version

Geotechnique

Centrifuge modelling of the influence of slope height on the seismic performance of rooted slopes

--Manuscript Draft--

Manuscript Number:	16-P-072R1
Full Title:	Centrifuge modelling of the influence of slope height on the seismic performance of rooted slopes
Article Type:	General Paper
Corresponding Author:	Jonathan Knappett, PhD University of Dundee Dundee, UNITED KINGDOM
Corresponding Author's Institution:	University of Dundee
Order of Authors:	Teng Liang, BEng PhD
	Jonathan Knappett, MA MEng PhD
Corresponding Author's Secondary Institution:	
Order of Authors Secondary Information:	
Manuscript Region of Origin:	UNITED KINGDOM
Abstract:	This paper presents an investigation into the influence of slope height on the role of vegetation to improve seismic slope stability. Dynamic centrifuge modelling was used to test six slope models with identical soil properties and model slope geometry within different centrifugal acceleration fields (10-g and 30-g, respectively) representing 1:10 and 1:30 scale slopes, i.e. slopes of different height at prototype scale. A 3-D root cluster analogue representing a tap-root system, with root area ratio (RAR), root distribution and root length representative of a 1:10 and 1:30 scale tree root cluster (of rooting depth 1.5 m at prototype scale) was modelled using 3-D printing techniques. A sequence of earthquake ground motions was applied to each model. The influences of filtering out low frequency components of the earthquake motion, such as was necessitated at the lowest scaling factor due to the practical limitations of the earthquake simulator, on dynamic amplification of motions within the slopes and the seismically induced slip, were firstly revealed. Subsequently, the effects of slope height on acceleration and deformation response of vegetated slopes were illustrated. It was found that the beneficial effects of roots on improving the seismic performance varied with the height of the slope. As an individual engineering technique for slope stabilisation, root reinforcement will not be such an effective solution for taller slopes and complementary hard engineering methods (e.g. piles, retaining walls) will be necessary. But for slopes of smaller heights (e.g. low height embankments along transport infrastructure), vegetation appears to represent a highly effective method of reducing seismic slip. Words: 5838 (excl. Abstract, notation & references) Figures: 16 Tables: 4
Suggested Reviewers:	Jason DeJong University of California at Davis jdejong@ucdavis.edu Prof. DeJong workd in the area of improving seismic performance by biological means.
	Gopal Madabhushi University of Cambridge mspg1@cam.ac.uk Prof. Madabhushi is an expert on centrifuge modelling of earthquake problems.
Opposed Reviewers:	
Additional Information:	

Question	Response
Please enter the total number of words in the main text only. The main text of the paper should be as concise as possible. The word count of General Papers should not exceed 5000 words and for Technical Notes should not exceed 2000 words. The word count of a submission excludes the abstract, list of notation, acknowledgements, references, tables and figure captions. Discussions, Book Reviews, and Obituaries should be less than 1000 words. Whilst Geotechnique reserves the right to publish papers of any length Authors should be aware that any submission for a General Paper that is significantly over the word limit will be subjected to pre-assessment and may be returned to the Authors for editing prior to being sent for review. The word limit for Technical Notes will be strictly adhered to, and if over 2000 words, the submission will be considered as a General Paper.	5838
Have you included a full notation list including definitions (and SI units of measurement where appropriate) for any mathematical terms and equations included in your paper?	Yes
Have you included a completed copyright transfer form? This is required for all publications and can be found here.	Yes
Have you uploaded each of your figures separately and in high-resolution .tiff (ideal for photographs) or .eps files (best for line drawings)? This is required for all figures before your paper can be accepted. Our figure requirements can be found here.	Yes
Have you uploaded your tables in an editable Microsoft Word (.doc) format?	Yes
Have you included a separate list of all your figure and table captions?	Yes
Are your figures clear when printed in black and white? (For example, are plot lines distinguishable; are tints sequentially graded?) As this journal is printed in black and white, any figures that are unclear may be removed.	Yes
Are your references in Harvard style? Our reference guidelines can be found here.	Yes
To ensure your paper is indexed correctly – and therefore as discoverable as possible – in our ICE Virtual Library,	Centrifuge modelling; Dynamics; Earthquakes; Slopes; Vegetation

please choose up to 6 keywords from our Keywords List. This can be found here. We are unable to accept keywords that do not appear on this list.	
Manuscript Classifications:	Centrifuge; Dynamic ground behaviour; Earthquake engineering; EARTHWORKS, EXCAVATION & FILL; LANDSLIDES AND SLOPE STABILITY; PHYSICAL MODELLING; Slope stability; SOIL DYNAMICS; Soil slope stabilisation
Author Comments:	No additional comments.

Centrifuge modelling of the influence of slope height on the seismic performance of rooted slopes

T.LIANG[1] and J.A.KNAPPETT[2]

[1] BEng PhD; Post-doctoral Research Associate, University of Dundee, UK

[2] MA MEng PhD; Reader in Civil Engineering, University of Dundee, UK

ABSTRACT

This paper presents an investigation into the influence of slope height on the role of vegetation to improve seismic slope stability. Dynamic centrifuge modelling was used to test six slope models with identical soil properties and model slope geometry within different centrifugal acceleration fields (10-g and 30-g, respectively) representing 1:10 and 1:30 scale slopes, i.e. slopes of different height at prototype scale. A 3-D root cluster analogue representing a tap-root system, with root area ratio (RAR), root distribution and root length representative of a 1:10 and 1:30 scale tree root cluster (of rooting depth 1.5 m at prototype scale) was modelled using 3-D printing techniques. A sequence of earthquake ground motions was applied to each model. The influences of filtering out low frequency components of the earthquake motion, such as was necessitated at the lowest scaling factor due to the practical limitations of the earthquake simulator, on dynamic amplification of motions within the slopes and the seismically induced slip, were firstly revealed. Subsequently, the effects of slope height on acceleration and deformation response of vegetated slopes were illustrated. It was found that the beneficial effects of roots on improving the seismic performance varied with the height of the slope. As an individual engineering technique for slope stabilisation, root reinforcement will not be such an effective solution for taller slopes and complementary hard engineering methods (e.g. piles, retaining walls) will be necessary. But for slopes of smaller heights (e.g. low height embankments along transport infrastructure), vegetation appears to represent a highly effective method of reducing seismic slip.

KEYWORDS: centrifuge modelling; dynamics; earthquakes; slopes; vegetation

INTRODUCTION

Previous experimental and analytical studies have led to a good understanding of root-soil interaction during soil slippage in the past 40 years (e.g Wu, 1976; Pollen and Simon, 2005; Wu, 2013). However, in contrast with this, relatively few studies have been performed on the global performance of vegetated slopes (Sonnenberg et al., 2011). Studies have generally explored reinforcement by vegetation in one of three ways. Plane-strain numerical models are most common, either through simulating the rooted zone as a soil-like continuum with additional apparent cohesion $c_r^{'}$ (e.g. Frydman & Operstein, 2001; Mao et al., 2014), or through treating roots as straight beams or anchor elements embedded into the continuum elements of the slope (e.g. Genet et al., 2008; Lin et al., 2010). However, as indicated by Stokes et al. (2014), such models are often not able to accurately predict the likelihood of landsliding as they are often based on oversimplified soil models and slope geometry and overlook spatial heterogeneity of the root reinforcement effect and the 3-D root group geometry. Large trials in the field

can overcome such disadvantages and provide a reliable insight into global slope behaviour (e.g. Brown, 1991; Smethurst et al., 2006; Smethurst et al., 2012; Smethurst et al., 2015). However, such trials are generally expensive and time consuming – as an example, it took 5 years to monitor the impacts of tree removal on a clay railway embankment as reported by Smethurst et al. (2015). Geotechnical centrifuge modelling can provide a balance between keeping expense low while maintaining a high level of fidelity and is therefore a good method for investigating the global performance of vegetated slopes.

During centrifuge model tests, roots have previously been modelled either using live plants (e.g. Sonnenberg et al., 2010; Askarinejad and Springman, 2015; Ng *et al.*, 2016) or root analogues with simple geometry (e.g. Sonnenberg et al., 2011; Eab et al., 2014; Liang et al., 2015). Real plants can potentially model both root mechanical and some hydrological effects, but are also highly variable, generally non-repeatable and can develop very different root morphology compared to field conditions (Ghestem et al., 2013). Root analogues have the advantage of high repeatability and are easily and quickly produced. The main issue with using such analogues is to find a material which simultaneously models the stiffness and strength of live roots (Liang et al., 2014). Liang et al. (2015) and Meijer et al. (2016) employed 3-D printed ABS plastic to fabricate root analogues with simplified geometry (namely, straight vertical or horizontal rods), and this approach provided substantially more representative properties compared to previously used analogue materials such as wood and rubber. Plate/ heart root systems of shrubs and trees, in which most of the roots behave independently, may be simplified into straight root groups (Stokes and Mattheck, 1996; Gary and Sotir, 1996; Liang et al., 2015). However, for deep tap root systems, for which the main tap root penetrates into the soil to significant depth and mobilises other attached roots to resist soil movement, it will not be appropriate to model them as straight root groups (Danjon et al., 2013) . A more sophisticated root model which can simulate realistic geometry of a deep tap root system is required, and 3-D printing offers an opportunity to achieve this.

Most previous studies have been concerned with studying failure under changes to the hydraulic conditions within the ground (e.g. Sonnenberg et al., 2010; Sonnenberg et al., 2011; Ng et al., 2016; Eab et al., 2014; Askarinejad and Springman, 2015). However Liang et al. (2015), for the first time, investigated the global behaviour of vegetated slopes subject to a sequence of earthquake ground motions, using straight root analogues as described above. The 1.5 m deep vegetation layer modelled appeared to act as a soft retaining wall, buttressing the movement of the slipping soil mass and significantly decreasing permanent settlement at the crest for the case of a 2.4 m high slope at prototype scale. For taller slopes having vegetation of a similar depth, it is unclear whether such a mechanism will still be active, or whether the failure mechanism may bypass the rooted zone.

To address the above issues, this paper discusses the results of a programme of dynamic centrifuge testing with the same model slope geometry (1:2 slope in sand) but performed at different scaling factors (1:10 and 1:30) and corresponding centrifugal acceleration fields (10-g and 30-g, respectively) subjected to a sequence of earthquake ground motions. The tests include both vegetated cases (using analogues, see below) and fallow benchmarks and all the vegetated cases have nominally the same rooted layer properties and geometry (1.5 m deep) at prototype scale. 3-D model root clusters with root area ratio (RAR), root distribution and root length representative of 1:10 and 1:30 geometrically-scaled models of the same tap-root system of a tree, were developed using 3-D printing techniques. The use of different scaling factors for representing different height

slope prototypes has implications for earthquake motion replication as the scaling factor for frequency, coupled with mechanical limitations of servo-hydraulic earthquake simulators, limits the low frequency content of the ground motions that can be controlled at smaller scaling factors (i.e. the 1:10 models herein). The seismic response of three fallow slope models is therefore investigated first to determine the effects of the frequency content of the earthquake motion on seismic ground motions and site/topographic amplification behaviour, and the permanent soil slip. This provides a benchmark for subsequent assessment of the comparative performance of rooted slopes of different heights, from which some recommendations for engineering practice are drawn.

DYNAMIC CENTRIFUGE MODELLING

Dynamic centrifuge modelling was conducted using the 3.5 m diameter beam centrifuge and servo-hydraulic earthquake simulator at the University of Dundee. A detailed description of this equipment can be found in Brennan et al. (2014). A total of 6 model slopes with identical overall geometry and soil properties were tested at different g-levels and with input motions with frequency contents as indicated in Table 1. All values presented herein are given at prototype scale, unless specifically noted otherwise. Typical model layouts are shown in Fig.1 for models TL 07 (a) and TL 06 (b). It should be noted here that the root cluster in Fig. 1(b) is shown simplified as a dotted circle for clarity.

Model preparation

The slope models were constructed within an Equivalent Shear Beam (ESB) container in order to replicate a semi-infinite horizontal boundary condition in the direction of shaking (Zeng and Schofield, 1996; Madabhushi and Teymur, 2003; Brennan et al., 2006; Haigh and Madabhushi, 2014). Further information on this specific container can be found in Bertalot (2013). The slopes (at model scale) were 240 mm tall from toe to crest, and were underlain by a further 80 mm of sand at the same relative density and had a slope angle of 27° (1:2). The root clusters (described in the following section) were hung at the specified positons shown and dry HST 95 Congleton silica sand was pluviated in air around the model roots to a relative density of I_D = 55%-60%. Fundamental properties of the sand are given in Table 2. Once the lower part of the root clusters was embedded in the soil, the lines used to hang the root clusters were cut off and removed. In this way, the root clusters most closely represented a ‘wished-in-place’ installation and therefore conservatively, may not represent small local (positive) changes to soil density/properties in the vicinity of roots growing into the soil in a field condition. ADXL78 micro-electromechanical system (MEMS) accelerometers (ACC) manufactured by Analog Devices were embedded inside each model to measure the horizontal accelerations within the soil specimen, and three external liner variable differential transformers (LVDTs) measuring settlement at the crest of the slope along the centreline and detecting any boundary effects (Madabhushi and Teymur, 2003). All slopes were tested dry to avoid the potential for the complicating effects of liquefaction. Further details on model preparation can be found in Liang (2015).

Model tree roots

Simplified 3-D root model clusters (Fig. 2) with root area ratio (RAR), root distribution and root length representative of a 1:10 and 1:30 geometrically-scaled tree root cluster consisting of a tap-root system was modelled. The root architecture used as a template was based on the tap root system of a white oak tree located at the Warnell School for Forestry and Natural Resources, University of Georgia, for which detailed characterisation of the root system had been undertaken (as reported in Danjon et al. 2008). Further details relating to the design process for this model can be found in Liang (2015). Willow, oak, poplar ,beech, alder and pine trees are some typical choices for the use of vegetation to stabilise slopes (Norris and Greenwood, 2006), though naturally vegetated slopes may have a much wider selection of species growing on them. There are very limited databases of detailed root system architecture of trees; the root system considered here grew in sloping ground and was therefore considered to be a suitable example root system for this study.

All of the roots except the tap root were simplified into circular curved rods and classified into different types (after Watson et al., 1995) based on their diameter, as shown in Table 3. The 3-D geometry can be seen in Fig. 1(a). The model root clusters produced were fabricated using the Stratesys Inc. uPrint SE Acrylonitrile Butadiene Styrene (ABS) rapid prototyper (known more commonly as a 3-D printer) at the University of Dundee following the procedures outlined in Liang et al. (2014), which discusses the 1:10 scale model. Compared with the 1:10 scale root cluster, the smallest model roots were eliminated in the 1:30 scale root cluster as shown in Table 3, due to the threshold minimum manufacturing size in the 3-D printer (0.75 mm in diameter). The corresponding differences in root distribution at prototype scale are shown in Fig. 3. The 3-D printing technique can generate a unidirectionally layered structure, which can successfully simulate the fibrous structure of tree roots. The layered ABS plastic root analogues were validated to be highly representative of the mechanical behaviour of real roots (in terms of Young's Modulus and tensile strength) after a series of uniaxial tension and bending tests, which is described in more detail in Liang et al. (2015).

The mean particle size of the sand used was 0.16 mm, while the minimum diameter of root segments modelled was 0.8 mm, which is only $6.7D_{50}$. Ovesen (1979) proposed that there was some deviation from continuum behaviour in centrifuge models when the ratio of foundation diameter to grain size was less than approximately 15 (Stone and Wood, 1992; Kutter, 1995). To verify what the impact of potential scale effects might be, a series of direct shear tests were conducted in a large direct shear apparatus (DSA, Fig. 4) with internal dimension of 300 mm × 300 mm × 270 mm, purpose-built for investigation of root-soil interaction. Further details about the advantage of such a large DSA compared with a conventional DSA for investigating rooted soil can be found in Liang (2015). The same 3D root clusters and density of soil as used in the centrifuge tests were used in the large DSA. The varied vertical confining stress for different potential slip plane locations in the centrifuge test was simulated in the DSA through altering the surcharge weight and varying the vertical position of the root cluster within the DSA. However, it should be noted that these tests are only indicative of the rooted soil shear strength at different depths within the centrifuge models as the trend of increasing confining stress with depth in the centrifuge tests could not truly be simulated, as demonstrated in Fig. 5(a). The DSA tests did however verify that the additional shear strength for both 1:30 and 1:10 scale root clusters were of the same order of magnitude and distribution with depth for the same applied effective stresses, as shown in Fig. 5(b). This suggested that there was a negligible particle size effect, despite the differences in model scale root analogue diameter at the different scales compared to the fixed median soil grain size in all tests.

Earthquake events

Earthquakes were simulated in-flight using the Actidyn QS67-2 servo-hydraulic earthquake simulator (EQS). The performance of this actuator is described in Brennan et al. (2014). Each slope model was subjected to eight successive earthquake motions (see Table 4), comprised of three different recordings with distinct peak ground acceleration (PGA), duration and frequency content. The motions used were recorded during the M_s=6.2 Aegion earthquake in 1995 (PGA=0.39g), the M_s=6.8 Northridge earthquake in 1994 (PGA=0.83g) and the M_s=6.3 L'Aquila earthquake in 2009 (PGA=0.33g). The three motions were downloaded from the PEER (Pacific Earthquake Engineering Research) Next Generation Attenuation model database and are shown as acceleration response spectra (ARS), normalised by the peak acceleration for the case of a system with nominal 5% damping in Fig. 6. All ARS reported subsequently in this paper are given at 5% damping, unless otherwise stated.

The motions were each band-pass filtered using an eighth-order Butterworth filter to obtain demand motions (see Fig.7) which were within the controllable range (40-300 Hz at model scale) of the EQS. At 1:10 scale this range is between 4 Hz and 30 Hz at prototype scale, while at 1:30 scale this range is between 1.33 Hz and 10 Hz. As mentioned above, significant differences in the seismic performance of slopes between these two scales may be expected due to the combined effects of different slope heights at prototype scale (hence different natural frequencies in the fundamental mode) and input motion frequency. Additionally, much of the energy associated with significant slip of the slope will be at low frequency, such that the overall magnitude of the permanent deformations in the 1:10 scale models may be expected to be much smaller than the 1:30 scale models. Evidence of this effect can also be seen in the significant differences in peak input acceleration between the two scales as shown in Table 4, and compared to the 'as-recorded' PGA values reported in the previous paragraph. A 'reduced' range at 1:30 scale of 4-10 Hz was therefore also introduced to provide both 1:10 scale and 1:30 scale models with the same amount of low frequency motion (< 4 Hz) filtered out in each case, so that a comparison could be made where only the slope height was different in the fallow case. It should be noted here than the frequency ranges between those two models are still not the same, but the higher frequency components (above 10 Hz) are not expected to be important for slip of the slope.

All motions were initially calibrated on a dummy slope model identical to Fig.1, but without instrumentation before formal testing to obtain repeatable achieved motions as close as possible to the filtered demand motions.

Natural frequency of the model slopes

The natural frequency (f_0) of the model slopes was estimated using:

$$f_0 = V_s / kH \qquad (1)$$

where V_s is the average shear wave velocity, H is the soil layer height (here, the slope height) and k is a coefficient for the shape of the soil layer (k = 4 for a semi-infinite horizontal layer; k = 2.61 for a triangular shaped layer, such as a slope (Gazetas, 1992)). In this study, no resonant column (RC) tests were performed, but

the shear wave velocity can be estimated based on the maximum shear modulus (G_0) at small strain below the elastic threshold:

$$G_0 = \rho V_s^2 \qquad (2)$$

where ρ is the density of the soil. Given the round shape of the particles (R= 0.53) of the HST 95 sand used in this study (Lauder, 2010), G_0 was here estimated using the relationship based on void ratio (e) proposed by Hardin and Black (1966) for round-grained sand at stresses less than 96 kPa:

$$G_0 = 7060\ \frac{(2.12-e)^2}{1+e} \cdot \left(p_0^{'}\right)^{3/5} \qquad (3)$$

where $p_0^{'}$ is the initial mean effective confining stress ,which can be expressed as:

$$p_0^{'} = \frac{(1+2K_0)\sigma_v^{'}}{3} \qquad (4)$$

where $\sigma_v^{'}$ is the average vertical effective stress and K_0 is the earth pressure coefficient at rest, which was estimated using:

$$K_0 = 1-\sin\phi^{'} \qquad (5)$$

where $\phi^{'}$ is the effective angle of friction. A value of $\phi^{'}$ =32° was reported by Al-Defae et al. (2013) for HST 95 sand, and was also used herein.

According to Eq (1)- Eq (5), the average natural frequency of the slope at 1:10 and 1:30 scale were estimated to be 13.9 Hz (0.07 s period) and 6.5 Hz (0.15 s period), respectively, and these values are shown with the demand motions in Fig 7.

SEISMIC PERFORMANCE OF FALLOW SLOPES

The seismic response of the fallow slopes under sequences of strong motion will be discussed first. This will provide a benchmark to subsequently assess the comparative performance of the rooted slopes.

Dynamic response – effect of frequency content of input motion

Comparing the 1:30 scale fallow models at reduced frequency range (TL-08) and at 'full' frequency range (TL-05) allows the same slope profile at prototype scale to be considered with the only difference being the amount of low frequency signal content contained within the ground motion. Comparison of the seismic performance of these two models was important to determine what the implications of a lack of low frequency content will be on slope behaviour, as was necessitated by the scaling factor used in the 1:10 scale tests.

A comparison of the peak acceleration amplification factor (S_{pk} = peak acceleration at a given depth divided by the peak acceleration of the input motion in the centrifuge tests) as a function of normalised elevation (z/H) of models TL 05 and TL08 is shown in Fig.8. Here, the first motion of each type was selected (i.e. EQ1, EQ2 and EQ5). Values suggested by Eurocode 8, Part 5 (BSI 2005b) for the crest (z/H = 1), are also included for comparison, where:

$$S_{pk} = S \cdot S_T \qquad (6)$$

where S is a soil factor describing the site effect. S= 1.4 for the 'ground type E ' soil in this study, as classified using Eurocode 8, Part 1 (BSI 2005a), and S_T is a topographic amplification factor of ≥ 1.2 for shallow slopes. The overall minimum amplification factor is therefore 1.7.

The response in the deeper soil (z/H < 0.2) is very similar in each case and includes a limited amount of attenuation for EQ2 and EQ5 which have the higher peak input acceleration, as previously observed by Ha et al. (2014). Towards the crest of the slope, the reduced motions EQ1 and EQ2 present much higher amplification factors with the exception of EQ5, which shows similar magnitude between the full and reduced motions. These findings are broadly in agreement with Fig. 7, given that the full versions of EQ1 and EQ2 consist of much low frequency (1.33-4 Hz) or high period content which was removed pre-test to fit the range of earthquake simulator, while EQ5 is mainly composed of higher frequency (lower period) components, hence showing less significant changes after filtering out low frequency components. This was further identified by examining dynamic amplification in the frequency domain via a transfer function, as shown in Fig. 9. The amplification at the crest is strongly frequency-dependent as evident in Fig.9 (a). Lower frequencies, below about 3 Hz, show a consistent amplification with a magnitude of less than 1.7, while at frequencies higher than 3 Hz, the amplification is seen to diverge but generally is much higher than 1.7. Such observations are consistent with the behaviour reported by Brennan and Madabhushi (2009). Therefore, filtering out the low frequency components (1.33-4 Hz) which have a lower amplification factor will result in a higher overall amplification factor for EQ1 and EQ2. Fig.10 shows a comparison of the spectral amplification factor (S_{amp}, given by dividing the crest spectral ordinates by those of input motion) between the same two models and shows that the S_{pk} values in Fig.8 are correlated with the difference in S_{amp} at periods above the natural period of the slope (i.e. low frequencies). Finally, it is apparent from Fig. 8(c) and Fig. 10(c) that the narrow-banded L'Aquila motion (EQ5-EQ7) is highly suitable for use in tests where different scaling factors are applied. The same is likely to be true of other motions with only limited low frequency (high period) content.

Dynamic response – effect of slope height

Having ascertained the impact of the input motion frequency content on the dynamic amplification within the slope, a comparison of tests TL-04 and TL-08 allows a comparison of two 1:2 slopes of different prototype heights, namely 2.4 m and 7.2 m, respectively, in each case with the same low frequency cut-off in the input motion (4 Hz). The ground motion at the crest for model TL 08 was observed to be generally larger than that of TL-04 for the same peak acceleration of the input motion. The variation of peak acceleration amplification factor with normalised elevation for these cases is shown in Fig.11. In two out of the three motions considered

(EQ1 and EQ2), the taller slope shows increased amplification compared to the shorter slope, up to or beyond 2.5 × the input motion peak. In all cases the amplification at the crest is significantly larger than the value of 1.7 suggested by EC8, but closer to the value of 2.1 (refer to Eq.6, $S_T = 1.5$) as suggested by Ashford et.al (2002) and Brennan and Madabhushi (2009). These observations would suggest that topographic amplification factors should be substantially increased, particularly in taller slopes.

Dynamic response – effect of aftershocks/preshocks

Fig.12 shows the recorded S_{pk} for the first and last earthquakes of similar type in test TL05 (i.e. for the tallest slope with 'full' frequency content). In this way it is possible to observe what the effect of previous strong ground motions is on the dynamic response of the slope in a subsequent event (i.e. in a strong aftershock). Generally the dynamic response of the ground was found to be insensitive to previous shaking, though by comparing each pair of like motions, a small amount of additional amplification can be seen in the later motion (e.g. compare EQ4 to EQ2 or EQ7 to EQ5). The effect is most apparent comparing EQ8 to EQ1 – these are both nominally the same motion, but EQ8 occurs after a significant amount of previous strong shaking. These observed small increases in amplification during later motions are presumably a result of densification of the soil outside of any slipping zone during previous strong shaking. If this is true, then in practical applications any effects of historical shaking may be captured through the site investigation and subsequent determination of the current state of the soil.

Permanent slope deformations

Fig. 13(a) shows a comparison of the permanent crest settlement across the eight earthquakes for model TL-05 and TL-08. It is found that in contrast to the dynamic motions within the main soil body (Fig. 8) the effect of removing the low frequency content of the input motion is highly significant for the permanent settlement at the crest. A reduction of 60% on permanent slope settlement was observed when the low frequency content between 1.33 Hz and 4 Hz was removed. Considering the response in terms of a Newmark sliding block analysis (Newmark, 1965), such low frequency components, having longer periods, would result in greater slip when they exceed the yield acceleration of the slope compared to higher frequency components of the same peak ground acceleration, due to the generation of larger slip velocities and hence, displacements. As a result, it is to be expected that these components will contribute the greater part of the accumulated slip.

A comparison of the permanent crest settlement across the eight earthquakes for models TL-04 and TL-08 (i.e. different height slopes with similar low frequency content) is shown in Fig. 13(b). An increase of approximately 175% on permanent slope settlement was observed when the height of the slope was increased from 2.4 m to 7.2 m. This ratio is broadly consistent with the increase in peak ground accelerations near the surface of the soil (the likely sliding mass) in the taller slopes (Fig.11) for the motions with significant low frequency content (EQ1 and EQ2) and can again be understood via the behaviour of a Newmarkian sliding system. If the two slopes, because of their identical slope angle, will both yield through the formation of a mechanism close to an infinite slope, then their yield acceleration will be the same (or at least similar). However,

the larger size of the ground motions with longer period components will mean that yield will be exceeded more often and with increased slip velocity (and hence, displacement) on each occasion, resulting in significantly increased slip.

The effects of preshocks and aftershocks on the deformations can also be evaluated for the full sequence of eight earthquake motions using Fig.13. As previously observed for similar fallow slopes by Al-Defae et al. (2013), the permanent slip in subsequent nominally identical ground motions reduces due to re-grading (geometric hardening through a reduction in slope angle with continued slip). This same effect can be observed in Fig.13 particularly comparing EQ2-EQ4 and EQ5-EQ7.

SEISMIC PERFORMANCE OF ROOTED SLOPES

Dynamic response

A comparison of shear modulus and damping as functions of cyclic shear strain within rooted and fallow slopes is shown in Fig.14. The data points were determined from second-order estimates using the accelerometer array at the crest of the slope following the method proposed by Brennan et al. (2005). They therefore represent the behaviour at slope mid-height. Some empirical models from the literature are also presented for comparison (Hardin and Drnevich, 1972; Ishibashi and Zhang, 1993; Oztoprak and Bolton, 2013). In the taller slopes (Fig. 14(b) and (c)) the shear modulus and damping at a given cyclic shear strain was highly similar between rooted and fallow slopes and this did not appear to be affected by the amount of low frequency content within the motion (though it can be seen that there is an increase in the maximum cyclic strain magnitude in the tests with greater low frequency content, TL05 and TL06). In the shorter slopes, the shear modulus appears to be reduced compared to the fallow case, while the damping is significantly higher (Fig. 15(a)). These two effects would tend to cancel each other out, and so the presence of the model roots in both cases would likely have a very limited effect on the overall dynamic behaviour of the soil.

To further investigate the dynamic response, ratios of peak acceleration (i.e. rooted/fallow) at the crest and locally within the rooted zone are shown in Fig. 15. A comparison of (a) and (b), where both cases have similar filtering-out of the low frequency components of the motion, shows that the roots locally reduce the amplitude of the dynamic ground motions in the smaller height slope (Fig. 15 (a)) while there is very little change in the larger height slope (Fig. 15(b)). Comparison of Fig. 15(b) to Fig. 15(c) suggests that there is little change locally whether or not there is significant low frequency content for a given slope height, as previously suggested by Fig. 14. Again considering these observations within a Newmarkian framework would suggest that in smaller height slopes, such as the 2.4 m high slope considered herein, the motions within the slipping mass of soil near the slope surface may be attenuated, potentially reducing accumulated seismic slip, while taller slopes (e.g. 7.2 m high slope here) may suffer larger slippage for a given ground motion as a result of negligible attenuation. This will be further discussed when discussing permanent deformations in the following section.

Although root systems may locally reduce acceleration magnitudes, affecting soil slip and permanent deformations, it is also important to understand how the overall dynamic motion at the crest of the slope may be affected by the presence of the roots, as this would represent the dynamic input that may be seen by

infrastructure located at the crest (e.g. if this were a transportation embankment). By examining the 'At crest' points in Fig. 15 it can be seen that in general the peak magnitude of the motion is unaffected by the presence of the roots, irrespective of whether there is local attenuation close to the rooted zone.

Permanent deformations

Fig. 16 shows a comparison of the permanent settlement at the crest of the slope between rooted and fallow cases. As observed for the fallow cases (Fig. 13), a decreasing trend of settlement was observed in the rooted slopes when subjected to successive strong motions (e.g. aftershocks) attributable to the aforementioned slope geometry change (re-grading). Reductions by 85% and 15% of the permanent fallow slope movement were observed due to the presence of the roots, for the 1:10 scale model (Fig. 16(a)) and 1:30 scale model (Fig. 16(b)), respectively. The majority of this reduction was observed in the first two motions (EQ1 and EQ2) for the 1:10 scale models which is consistent with previous observations of a simplified straight root analogue case representative of a plate / heart type root system previously reported by Liang et al. (2015). This is attributable to the rapid mobilisation of root-soil interaction due to the initial soil slip under dynamic loading. After the initial rapid mobilisation, the additional resistive force of the root was largely constant and associated with yielding of the soil around the roots.

Given that the root analogues at different scales had highly similar strengthening effects on the soil over the upper 1.5 m (Fig. 5), it is perhaps surprising that the 1:30 scale rooted model experienced a much lower reduction of crest settlement compared with 1:10 scale rooted model. To understand this behaviour, the Newmark sliding block framework can again be considered. Within this framework, the presence of the roots could feasibly reduce permanent slip in two ways: (i) by increasing the yield acceleration of the slope, either through a change of soil strength or a change of failure mechanism; or (ii) via a reduction of the dynamic motions within the slope (specifically near the surface in the sliding mass).

Fig. 15 has already provided some evidence for point (ii), namely that motions are attenuated somewhat in the smaller slope, unlike in the taller slope. In terms of point (i), Fig. 6 has shown that in both cases the root models add significant additional shear strength within their zone of influence, especially considering the low confining stresses within the soil over the top 1.5 m. Previously Al-Defae et al. (2013) determined that the shear plane in a fallow 1:2 slope formed of the same soil at the same relative density and for a similar height (H = 8 m, compared to H = 7.2 m for the 1:30 slope in this study) was at a depth of approximately 0.5 m and was of the translational/infinite type. Therefore it may be inferred that a translational failure will also be critical and at a similar depth in the smaller fallow 1:10 slope. The roots always have a positive contribution to shear strength at whatever depth the shear plane is (Fig. 5), until close to their tips, at which point the strength reverts to being provided by the soil only. Therefore it is highly likely that the optimal position of the shear plane associated with the critical failure mechanism over the central (majority) part of the slope will be pushed deeper, as it will be easier to shear through the unreinforced soil below the root tips, rather than through the quite extensively reinforced rooted zone. In the case of the 1:10 scale slope, this would result in significant changes to the geometry of the slip plane around the toe of the slope to form a kinematically admissible mechanism (refer to Fig. 1). Such changes to the mechanism geometry would be less severe in the case of the 1:30 slope (where the

root depth is only 21% of the slope height) and so it is likely that the yield acceleration of the smaller slope (root depth is 63% of *H* sufficient to induce a buttressing mechanism, Liang et al. 2015) will be increased by more than the taller slope. The cumulative effect of reduced dynamic motion and a higher yield acceleration may explain why the roots are apparently much more effective at reducing slip in the shorter slope; however, such a mechanism requires further investigation.

The centrifuge observations from this study, therefore potentially suggest that there may be a limiting height of slope (or height of slope as a function of rooting depth) beyond which other, more traditional forms of reducing slip (e.g. discretely spaced pile rows, Al-Defae and Knappett, 2014) may be more effective, but also that for slopes of modest height (e.g. small embankments) tree roots may be a highly effective method of improving seismic performance.

CONCLUSIONS

A series of centrifuge tests has been performed at different scales (1:10 and 1:30) and corresponding centrifugal acceleration fields (10-g and 30-g, respectively) to investigate the performance of slopes of different heights containing root analogues under a sequence of earthquake motions. The following principal conclusions can be drawn from the study:

a) Amplification factors for all cases were observed to be significantly larger than the minimum value of 1.7 suggested by EC8. These observations would suggest that topographic amplification factors should be substantially increased, particularly in taller slopes.

b) Filtering out the low frequency (high period) component of the motion, such as was necessitated by the low scaling factor during centrifuge modelling has a significant effect on dynamic amplification of motion within the slope when the frequency band is wide, but for narrow band motions with few low frequency components, such effect is very limited. Such motions would be highly suitable for use in centrifuge testing where different scaling factors are applied.

c) The dynamic response of the ground at the crest of the slope was found to be highly dependent on slope height and not represented by site and topographic amplification factors which are independent of slope height, as in current design codes. The dynamic response at the crest was also found to be largely insensitive to previous shaking and the presence of vegetation.

d) The influence of vegetation on permanent displacement appears to be strongly dependent on the height of the slope. In this study, smaller height vegetated slopes performed much better than taller slopes. This indicates that there may be a limiting height of slope beyond which other, more traditional forms of reducing seismic permanent deformation may be more effective. The reason for this appears to be a combination of reduced accelerations within the slipping mass and a more significant change in failure mechanism (and hence greater increase in yield acceleration) within the smaller slopes. This suggests that for slopes of modest height (e.g. long low height embankments along transport infrastructure), tree roots may be a very effective seismic slope stabilisation method. For soil conditions and slope geometries similar to those considered herein, it would appear that slopes < 5 m tall (rooting depth > 30% of slope height) will have their seismic performance substantially improved by the presence of roots.

Slopes taller than this or with shallower rooting depths are likely only to see a modest improvement to seismic performance, and may therefore require other methods of improving their perfromance (e.g. piling).

ACKNOWLEDGEMENTS

The authors would like to express their sincere gratitude to Gary Callon, Colin Stark and William Mark at the University of Dundee for their assistance in printing the model root analogues and undertaking the centrifuge test programme. The first author would like to acknowledge the financial support of the China Scholarship Council.

NOTATION

$c_r^{'}$	cohesion due to reinforcement
C_z	coefficient of uniformity
C_z	coefficient of curvature
D_{10}	particle diameter at which 10% is smaller
D_{30}	particle diameter at which 30% is smaller
D_{50}	particle diameter at which 50% is smaller
D_{60}	particle diameter at which 60% is smaller
e	void ratio
e_{max}	maximum void ratio
e_{min}	minimum void ratio
f_0	fundamental natural frequency
G_0	small strain shear modulus
G_s	specific gravity
$\boldsymbol{g}$	acceleration due to gravity(=9.81m/s^2)
H	soil layer (slope) height
I_D	relative density
k	coefficient for the shape of soli layer
K_0	coefficient of earth press at rest
M_s	surface wave magnitude
$p_0^{'}$	initial mean effective confining stress
S	Soil factor describing the site effect
S_T	topographic amplification factor

S_{pk}	peak acceleration amplification factor
R	particle roundness
V_s	average shear wave velocity
z	depth
γ	unit weight
γ_{max}	maximum unit weight
γ_{min}	minimum unit weight
ρ	density
$\sigma_v^{'}$	normal effective stress
$\phi^{'}$	effective angle of friction

REFERENCE

Al-Defae AH, Caucis K and Knappett JA , 2013. Aftershocks and the whole-life seismic performance of granular slopes. Géotechnique **63**(**14**): 1230–1244. doi:10.1680/geot.12.P.149.

Al-Defae AH and Knappett JA , 2014. Centrifuge Modeling of the Seismic Performance of Pile-Reinforced Slopes. Journal of Geotechnical and Geoenvironmental Engineering **140**(**6**): 1–13. doi:10.1061/(ASCE)GT.1943-5606.0001105.

Ashford SA, Sitar N and Asce M , 2002. Simplified Method for Evaluating Seismic Stability of Steep Slopes. Journal of Geotechnical and Geoenvironmental Engineering **128**(**2**): 119–128.

Askarinejad A and Springman SM , 2015. Centrifuge modelling of the effects of vegetation on the response of a silty sand slope subjected to rainfall. In *Computer Methods and Recent Advances in Geomechanics*. Taylor & Francis Group, London, UK. pp. , pp. 1339–1344.

Bertalot D , 2013. *Foundations on layered liquefiable soils*. PhD thesis,University of Dundee,UK.

Brennan AJ, Knappett JA, Loli M, et al. , 2014. Dynamic centrifuge modelling facilities at the University of Dundee and their application to studying seismic case histories. In *Proceedings of the 8th International Conference on Physical Modelling in Geotechnics, Perth, Australia*. vol. 1, 2014, pp. 227–233.

Brennan AJ and Madabhushi SPG , 2009. Amplification of seismic accelerations at slope crests. Canadian Geotechnical Journal **46**(**5**): 585–594. doi:10.1139/T09-006.

Brennan AJ, Madabhushi SPG and Houghton NE , 2006. Comparing laminar and equivalent shear beam (ESB) containers for dynamic centrifuge modelling. In *Proceedings of the 6th International Conference on Physical Modelling in Geotechnics, Hong Kong, China*. vol. 1–2, 2006, pp. 171–176.

Brennan AJ, Thusyanthan NI and Madabhushi SPG , 2005. Evaluation of shear modulus and damping in dynamic centrifuge tests. Journal of Geotechnical and Geoenvironmental Engineering **131**(**12**): 1488–1497. doi:10.1061/(ASCE)1090-0241(2005)131:12(1488).

Brown WJ , 1991. Landslide control on North Island, New Zealand. Geographical Review **81**(**4**): 457–472.

BSI , 2005a. *Eurocode 8: Design of stuctures for earthquake resistance -part 1: General rules,seismic actions and rules for buildings, EN 1998-5:2004. Bristish Standard Institution, UK*.p.

BSI , 2005b. *Eurocode 8: Design of stuctures for earthquake resistance -part 5: Foundations,retaining strctures and geotechincal aspects, EN 1998-5:2004. Bristish Standard Institution, UK*.p.

Danjon F, Barker DH, Drexhage M and Stokes A , 2008. Using three-dimensional plant root architecture in models of shallow-slope stability. Annals of Botany **101**(**8**): 1281–1293. doi:10.1093/aob/mcm199.

Danjon F, Khuder H and Stokes A , 2013. Deep phenotyping of coarse root architecture in R. Pseudoacacia reveals that tree root system plasticity is confined within its architectural model. PLoS ONE **8**(**12**): e83548. doi:10.1371/journal.pone.0083548.

Eab K, Takahashi A and Likitlersuang S , 2014. Centrifuge modelling of root-reinforced soil slope subjected to rainfall infiltration. Géotechnique Letters **4**: 211–216. doi:10.1680/geolett.14.00029.

Frydman S and Operstein V , 2001. Numerical simulation of direct shear of rootreinforced soil. Proceedings of the ICE - Ground Improvement **5**(**1**): 41–48. doi:10.1680/grim.2001.5.1.41.

Gary DH and Sotir RB , 1996. *Biotechnical and Soil Bioengineering Slope Stabilization: A Practical Guide for Erosion Control.* John Wiley & Sons, New York.

Gazetas G and Dakoulas P , 1992. Seismic analysis and design of rockfill dams: state-of-the-art. Soil Dynamics and Earthquake Engineering **11**: 27–61.

Genet M, Kokutse N, Stokes A, et al. , 2008. Root reinforcement in plantations of Cryptomeria japonica D. Don: effect of tree age and stand structure on slope stability. Forest Ecology and Management **256**(**8**): 1517–1526. doi:10.1016/j.foreco.2008.05.050.

Ghestem M, Veylon G, Bernard A, et al. , 2013. Influence of plant root system morphology and architectural traits on soil shear resistance. Plant and Soil **377**(**1**–**2**): 43–61. doi:10.1007/s11104-012-1572-1.

Ha JG, Lee SH, Kim DS and Choo YW , 2014. Simulation of soil-foundation-structure interaction of Hualien large-scale seismic test using dynamic centrifuge test. Soil Dynamics and Earthquake Engineering **61**–**62**: 176–187. doi:10.1016/j.soildyn.2014.01.008.

Haigh SK and Madabhushi SPG , 2014. Discussion of ‘ Performance of a transparent fl exible shear beam container for geotechnical centrifuge modelling of dynamic problems by Ghayoomi , Dashti and McCartney ’. Soil Dynamics and Earthquake Engineering **67**: 359–362. doi:10.1016/j.soildyn.2014.02.003.

Hardin BO and Black WL , 1966. Sand stiffness under various triaxial stresses. Journal of the Soil Mechanics and Foundations Division **92**(**2**): 27–42.

Hardin BO and Drnevich VP , 1972. Shear Modulus and Damping in Soils: Design Equations and Curves. Journal of the Soil Mechanics and Foundations Division **98**(**7**): 667–692.

Ishibashi I and Zhang X , 1993. Unified dynamic shear moduli and damping patios of sand and clay. Soil and Foundations **33**(**1**): 182–191. doi:10.3208/sandf1972.33.182.

Kutter B , 1995. Recent Advances in Centrifuge Modeling of Seismic Shaking. In *Proceedings of the Third International Conference on Recent Advances in Geotechnical Earthquake Engineering and Soil Dynamics, St.Louis, Missouri*. vol. 2, 1995, pp. 927–941.

Lauder K , 2010. *The performance of pipeline ploughs*. PhD thesis,University of Dundee,UK.

Lees A , 2013. Seasonal slope movements in an old clay fill embankment dam. Canadian Geotechnical Journal **50**(**5**): 503–520. doi:10.1139/cgj-2012-0356.

Liang T , 2015. *Seismic performance of vegetated slopes*. PhD thesis,University of Dundee,UK.

Liang T, Knappett JA and Bengough AG , 2014. Scale modelling of plant root systems using 3-D printing. In *Proceedings of the 8th International Conference on Physical Modelling in Geotechnics, Perth, Australia*. vol. 1, 2014, pp. 361–366.

Liang T, Knappett JA and Duckett N , 2015. Modelling the seismic performance of rooted slopes from individual root–soil interaction to global slope behaviour. Géotechnique **65**(**12**): 1–15. doi:10.1680/geot.14.P.207.

Lin DG, Huang BS and Lin SH , 2010. 3-D numerical investigations into the shear strength of the soil-root system of Makino bamboo and its effect on slope stability. Ecological Engineering **36**(**8**): 992–1006. doi:10.1016/j.ecoleng.2010.04.005.

Madabhushi SPG and Teymur B , 2003. Experimental study of boundary effects in dynamic centrifuge modelling. Géotechnique **53**(**7**): 655–663. doi:10.1680/geot.2003.53.7.655.

Mao Z, Bourrier F, Stokes A and Fourcaud T , 2014. Three-dimensional modelling of slope stability in heterogeneous montane forest ecosystems. Ecological Modelling **273**: 11–22. doi:10.1016/j.ecolmodel.2013.10.017.

Meijer GJ, Bengough AG, Knappett JA, et al. , 2016. New in situ techniques for measuring the properties of root-reinforced soil – laboratory evaluation. Geotechnique **66**(**1**): 27–40.

Newmark NM , 1965. Effects of Earthquakes on Dams and Embankments. Géotechnique **15**(**2**): 159–160. doi:10.1680/geot.1965.15.2.139.

Ng CWW, Leung AK, Yu R and Kamchoom V , 2016. Hydrological Effects of Live Poles on Transient Seepage in an Unsaturated Soil Slope: Centrifuge and Numerical Study. Journal of Geotechnical and Geoenvironmental Engineering : 4016106. doi:10.1061/(ASCE)GT.1943-5606.0001616.

Norris J and Greenwood J , 2006. Assessing the role of vegetation on soil slopes in urban areas. IAEG, paper (**744**): 1–12.

Ovesen NK , 1979. The measurement, selection, and use of design parameters in geotechnical engineering. In *Proceeding of the 7th European Conference of Soil Mechanics and Foundation Engineering,Brighton,*

England. vol. 4, 1979, pp. 319–323.

Oztoprak S and Bolton MD , 2013. Stiffness of sands through a laboratory test database. Géotechnique **63**(**1**): 54–70. doi:10.1680/geot.10.P.078.

Pollen N and Simon A , 2005. Estimating the mechanical effects of riparian vegetation on stream bank stability using a fiber bundle model. Water Resources Research **41**(**7**): 1–11. doi:10.1029/2004WR003801.

Smethurst JA, Briggs KM, Powrie W, et al. , 2015. Mechanical and hydrological impacts of tree removal on a clay fill railway embankment. Geotechnique **65**(**11**): 869–882.

Smethurst J, Clarke D and Powrie W , 2012. Factors controlling the seasonal variation in soil water content and pore water pressures within a lightly vegetated clay slope. Geotechnique **62**(**5**): 429–446.

Smethurst J, Clarke D and Powrie W , 2006. Seasonal changes in pore water pressure in a grass covered cut slope in London clay. Geotechnique **56**(**8**): 523–537. doi:10.1680/geot.2006.56.8.523.

Sonnenberg R, Bransby MF, Bengough AG, et al. , 2011. Centrifuge modelling of soil slopes containing model plant roots. Canadian Geotechnical Journal **49**(**1**): 1–17. doi:10.1139/T11-081.

Sonnenberg R, Bransby MF, Hallett PD, et al. , 2010. Centrifuge modelling of soil slopes reinforced with vegetation. Canadian Geotechnical Journal **47**(**12**): 1415–1430. doi:10.1139/T10-037.

Stokes A and Mattheck C , 1996. Variation of wood strength in tree roots. Journal of Experimental Botany **47**(**298**): 693–699. doi:10.1093/jxb/47.5.693.

Stones KJL and Wood DM , 1992. Effects of dilatancy and particle size observed in model tests on sand. Soil and Foundations **32**(**4**): 43–57.

Watson A, Marden M and Rowan D , 1995. Tree Species Performance and Slope Stability. In *Vegetation and Slopes*. Thomas Telford, London, UK. pp. , pp. 161–171.

Wu TH , 1976. Investigation of Landslides on Prince of Wales Island, Alaska. Geotechnical Engineering Report 5. Civil Engineering Department, Ohio State University, Columbus, Ohio, USA

Wu TH , 2013. Root reinforcement of soil: review of analytical models, test results, and applications to design. Canadian Geotechnical Journal **50**(**3**): 259–274.

Zeng X and Schofield AN , 1996. Design and performance of an equivalent-shear-beam container for earthquake centrifuge modelling. Géotechnique **46**(**1**): 83–102. doi:10.1680/geot.1996.46.1.83.

Table1. Summary of centrifuge models tested

Test identification number	Test scale	Slope height (m)	Root type	root cluster quantity	Motion frequency content (Hz)
TL 04	1:10	2.4	Fallow	0	4-30
TL 05	1:30	7.2	Fallow	0	1.33-10
TL 06	1:30	7.2	1:30 scale root cluster	36	1.33-10
TL 07	1:10	2.4	1:10 scale root cluster	4	4-30
TL 08	1:30	7.2	Fallow	0	4-10
TL 09	1:30	7.2	1:30 scale root cluster	36	4-10

Table2. State-independent physical properties of HST95 silica sand (After Lauder, 2010)

Property	Value
Specific gravity, G_s	2.63
D_{10}:mm	0.09
D_{30}:mm	0.12
D_{50}:mm	0.16
D_{60}:mm	0.17
C_u	1.9
C_z	1.06
Maximum void ratio, e_{max}	0.769
Maximum void ratio, e_{min}	0.467

Table 3. Root diameter class for medium and structural roots (not including tap root)

Diameter at 1:10 model scale (mm)	Number of roots	Diameter at1:30 model scale (mm)	Number of roots	Diameter range at prototype scale (mm)	Root class at prototype scale (after Watson et al. 1995)
-	-	-	-	<5	fine
0.8	109	-	-	5-10	small
1.6	81	0.8	81	10-20	medium
3	43	1	43	20-40	large
5	13	1.6	13	>40	coarse

Table4. Sequence of input motions

Motion ID	Input motion	Peak input acceleration: a_g (**g**)		
		4-30 Hz	1.33-10 Hz	4-10 Hz
EQ1	Aegion,1995	0.12	0.21	0.15
EQ2	Northridge,1994	0.28	0.64	0.29
EQ3	Northridge,1994	0.28	0.64	0.29
EQ4	Northridge,1994	0.28	0.64	0.29
EQ5	L'Aquila,2005	0.23	0.27	0.29
EQ6	L'Aquila,2005	0.23	0.27	0.29
EQ7	L'Aquila,2005	0.23	0.27	0.29
EQ8	Aegion,1994	0.12	0.21	0.15

Fig.1: Schematic of centrifuge model geometry, instrumentation and position of root analogues: (a) 1:10 scale model; (b) 1:30 scale mode (Dimensions at prototype scale in meters).

Fig.2: ABS plastic root models produced from 3-D printer showing the size difference between 1:10 scale and 1:30 scale models. Horizontal lines indicate potential shear plane depths at prototype scale.

Fig.3: 2D distribution of roots intersecting four planes at different depths below the ground surface (as shown in Fig. 2) for 3-D root models at prototype scale: (a) 1:10 scale; (b) 1:30 scale (downslope positive).

Fig.4: Schematic of large direct shear apparatus (DSA) – 1:10 scale model root cluster shown.

Fig.5: Comparison of DSA test results for 1:10 and 1:30 scale root clusters (depths at prototype scale): (a) variation of confining stress with depth; (b) additional shear strength provided by roots.

Fig.6: Normalised acceleration response spectra (ARS) of input motions as recorded in the field.

Fig.7: Normalised ARS of filtered input motions for centrifuge testing: (a) Aegion; (b) Northridge; (c) L'Aquila.

Fig.8: Comparison of peak acceleration amplification between 'full' and reduced frequency content input motions at 1:30 scale: (a) in EQ1 (Aegion); (b) in EQ2 (Northridge); (c) in EQ5 (L'Aquila).

Fig.9: Acceleration amplification factor in the frequency domain: (a) 1:30 scale model at full frequency content; (b) 1:30 scale model at reduced frequency content.

Fig.10: Comparison of ARS-derived amplification factor between 1:30 scale models at full and reduced frequency content: (a) in EQ1; (b) in EQ2; (c) in EQ5.

Fig.11: Effect of slope height on peak acceleration amplification: (a) in EQ1; (b) in EQ2; (c) in EQ5.

Fig.12: Increased peak ground motion amplification in aftershocks, 1:30 scale fallow model (TL 05) shown.

Fig.13: Comparison of permanent settlement at the crest in fallow slopes: (a) effect of input motion frequency content; (b) effect of slope height.

Fig.14: Comparison of shear modulus degradation and damping between fallow and root reinforced slopes: (a) 1:10 scale models; (b) 1:30 scale models at reduced frequency content; (c) 1:30 scale models at full frequency content.

Fig.15: Reduction in peak acceleration due to the presence of roots: (a) 1:10 scale model; (b) 1:30 scale model at reduced frequency content; (c) 1:30 scale model at full frequency content.

Fig.16: Comparison of permanent crest settlements between fallow and root-reinforced slopes: (a) 1:10 scale models; (b) 1:30 scale models at reduced frequency content; (c) 1:30 scale models at full frequency content.

Figure 1a

Click here to download Figure Fig1a_R1.tif

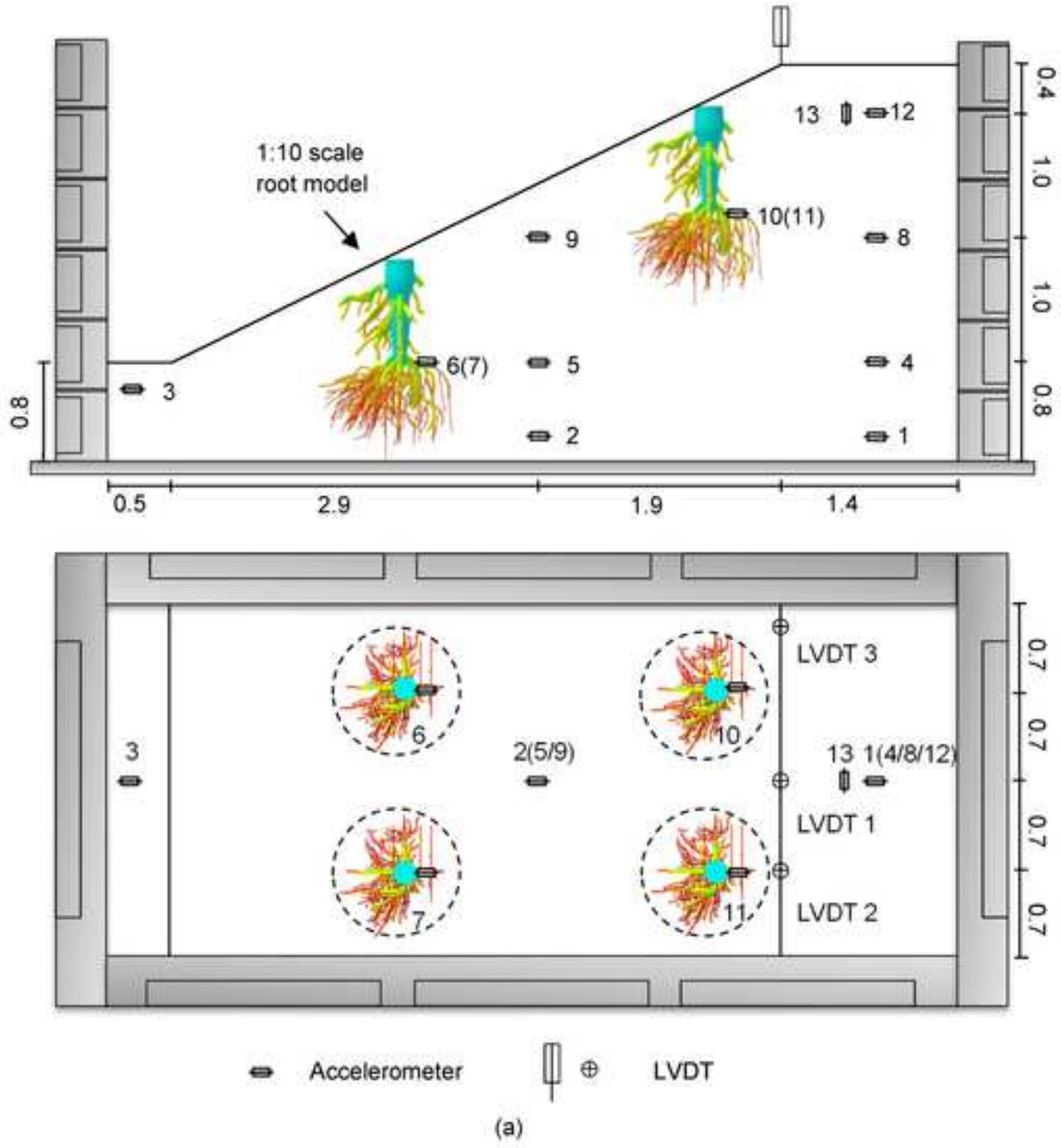

(a)

Figure 1b

Click here to download Figure Fig1b_R1.tif

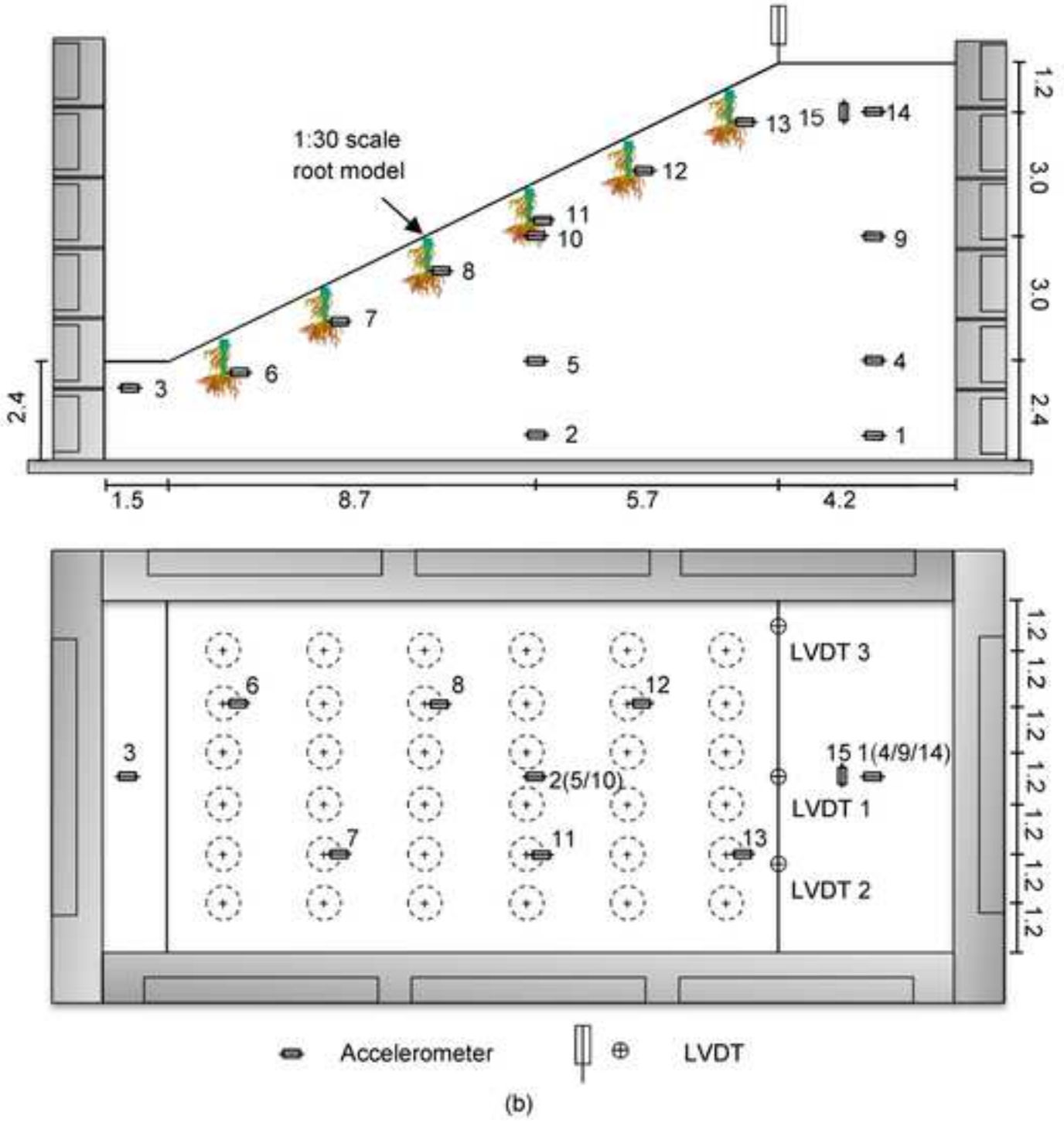

(b)

Figure 2

Click here to download Figure Fig2_R1.tif

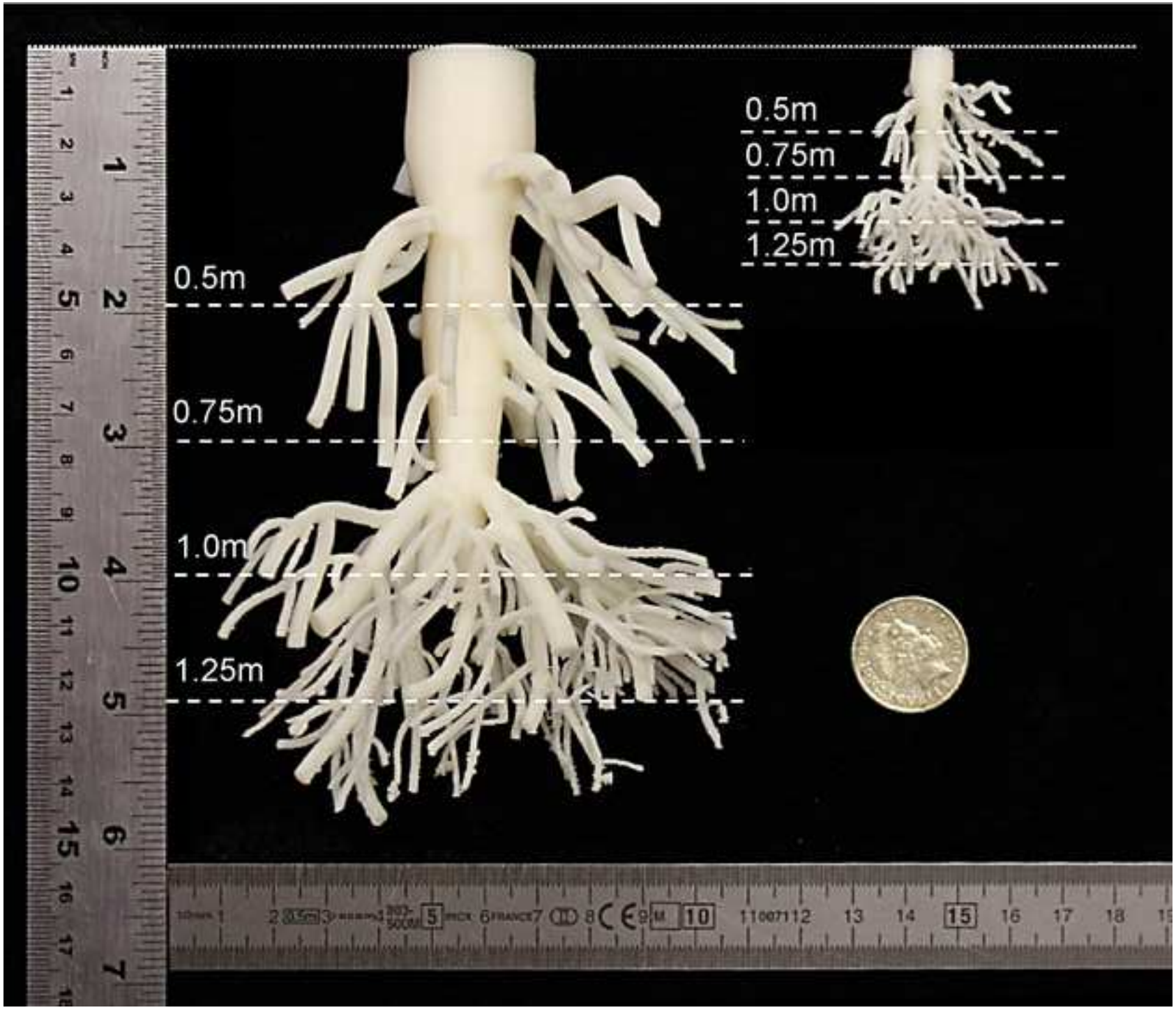

Figure 3a

Click here to download Figure Fig3a_R1.tif

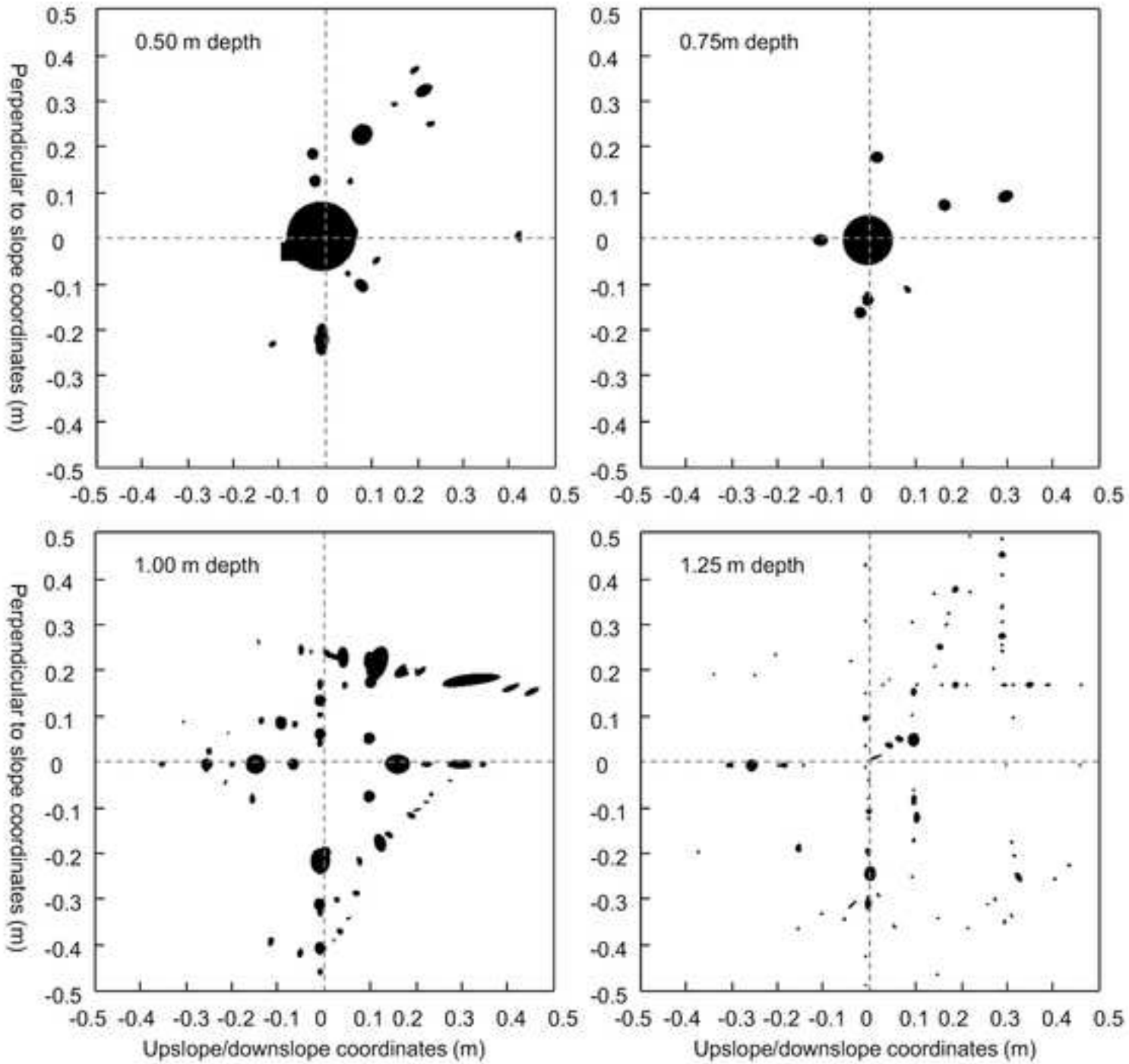

Figure 3b

Click here to download Figure Fig3b_R1.tif

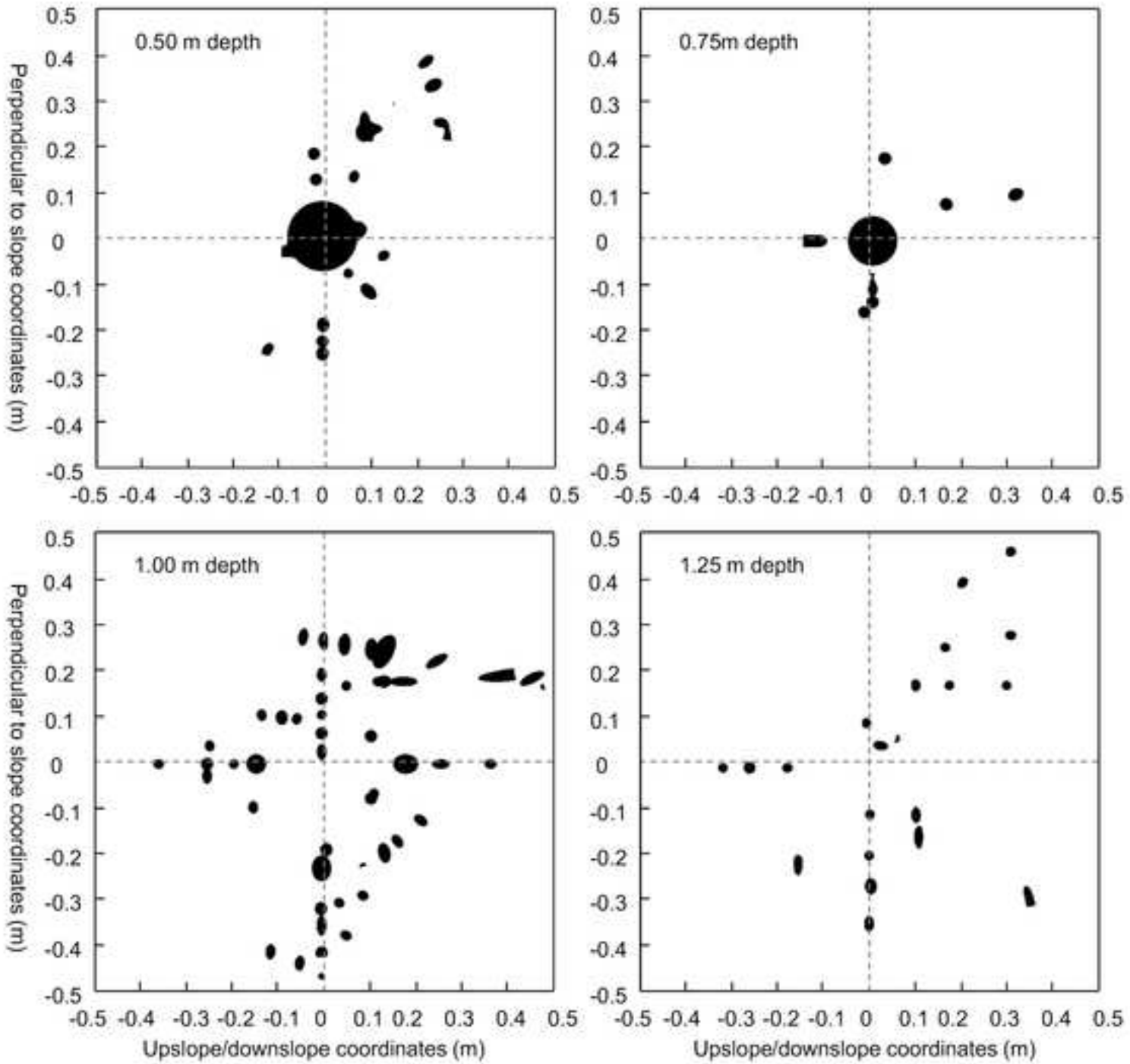

Figure 4

Click here to download Figure Fig4_R1.tif

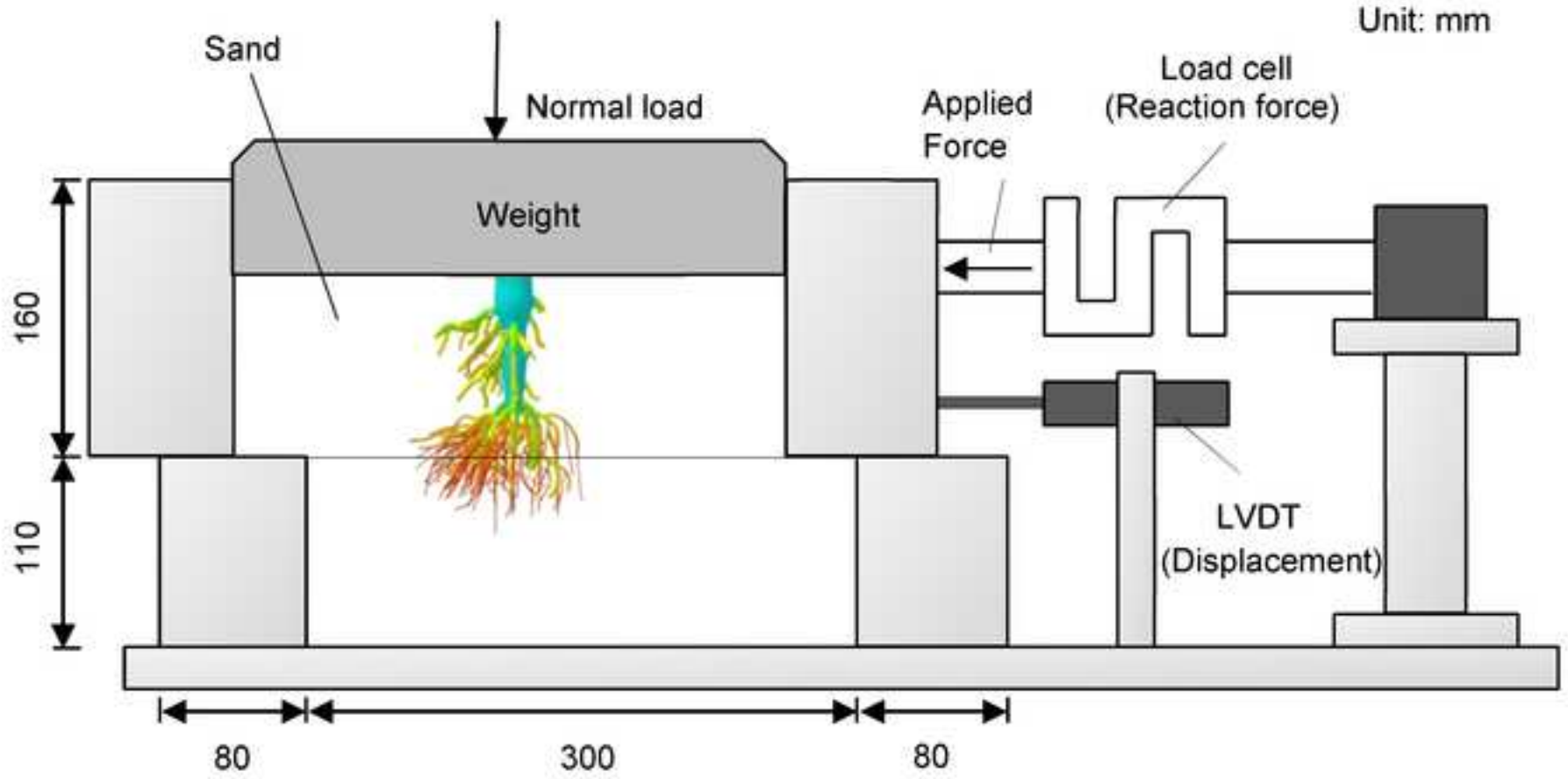

(b)

Figure 5

Click here to download Figure Fig5_R1.TIF

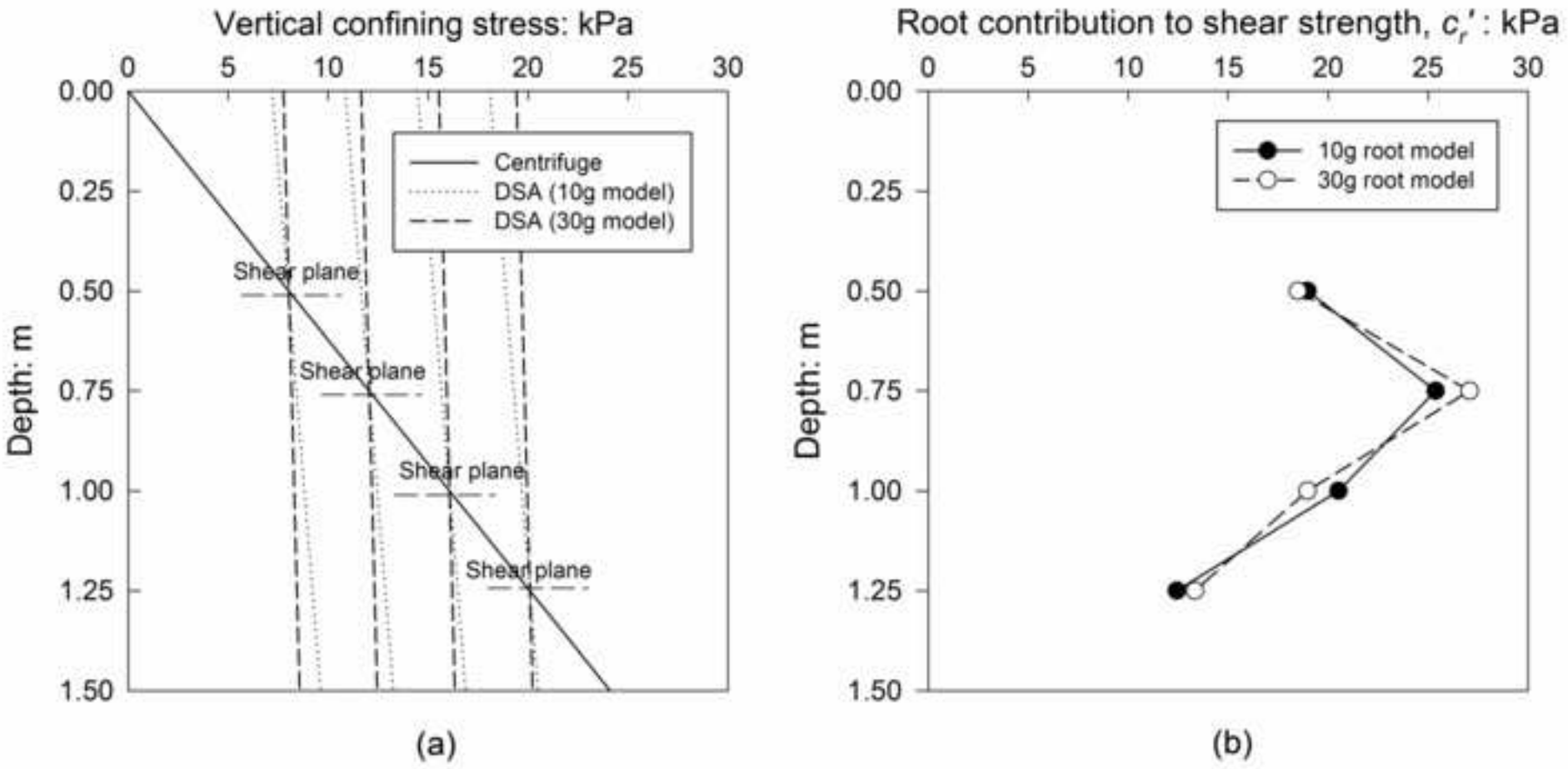

Figure 6

Click here to download Figure Fig6_R1.TIF

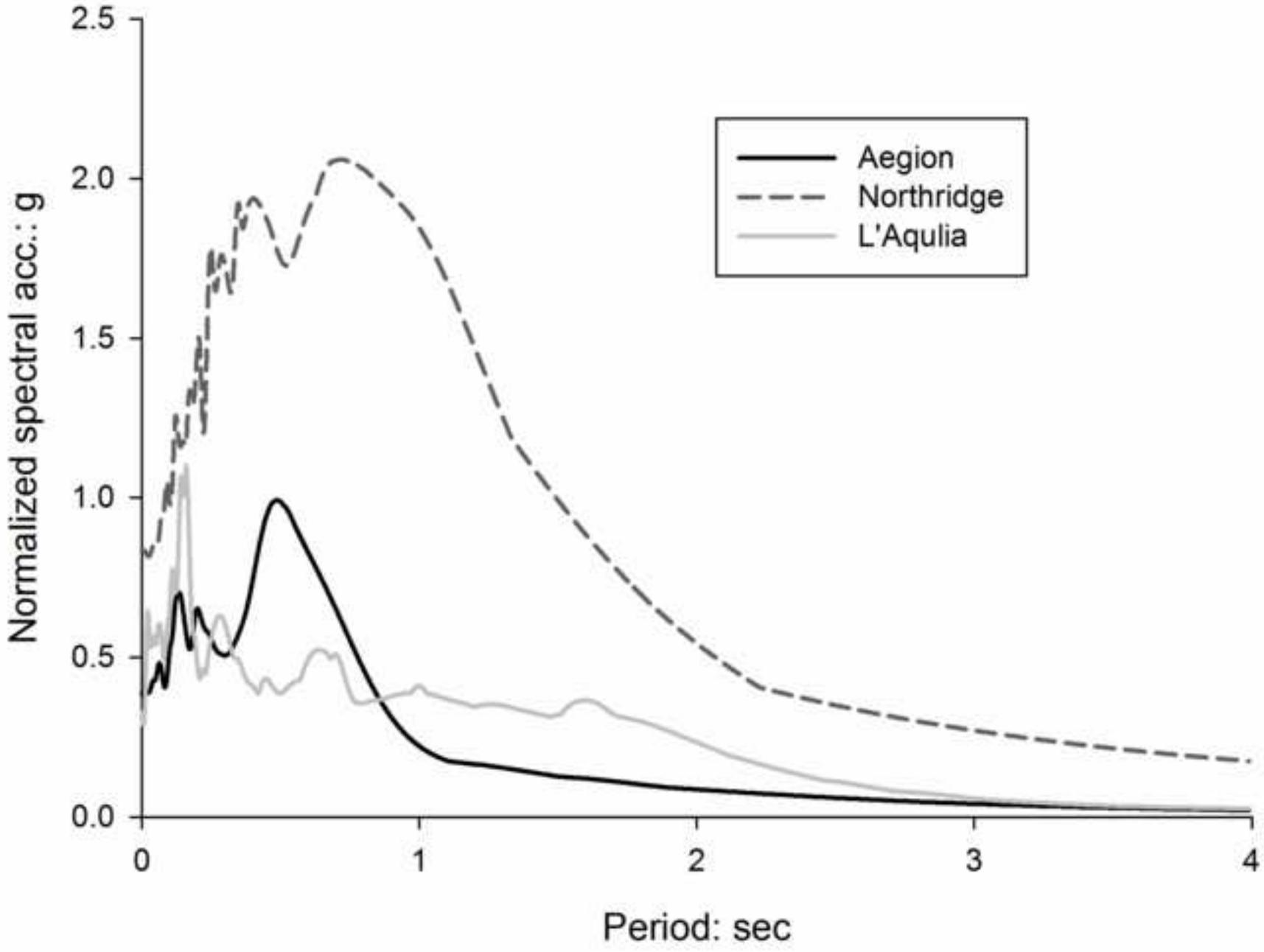

Figure 7

Click here to download Figure Fig7_R1.TIF

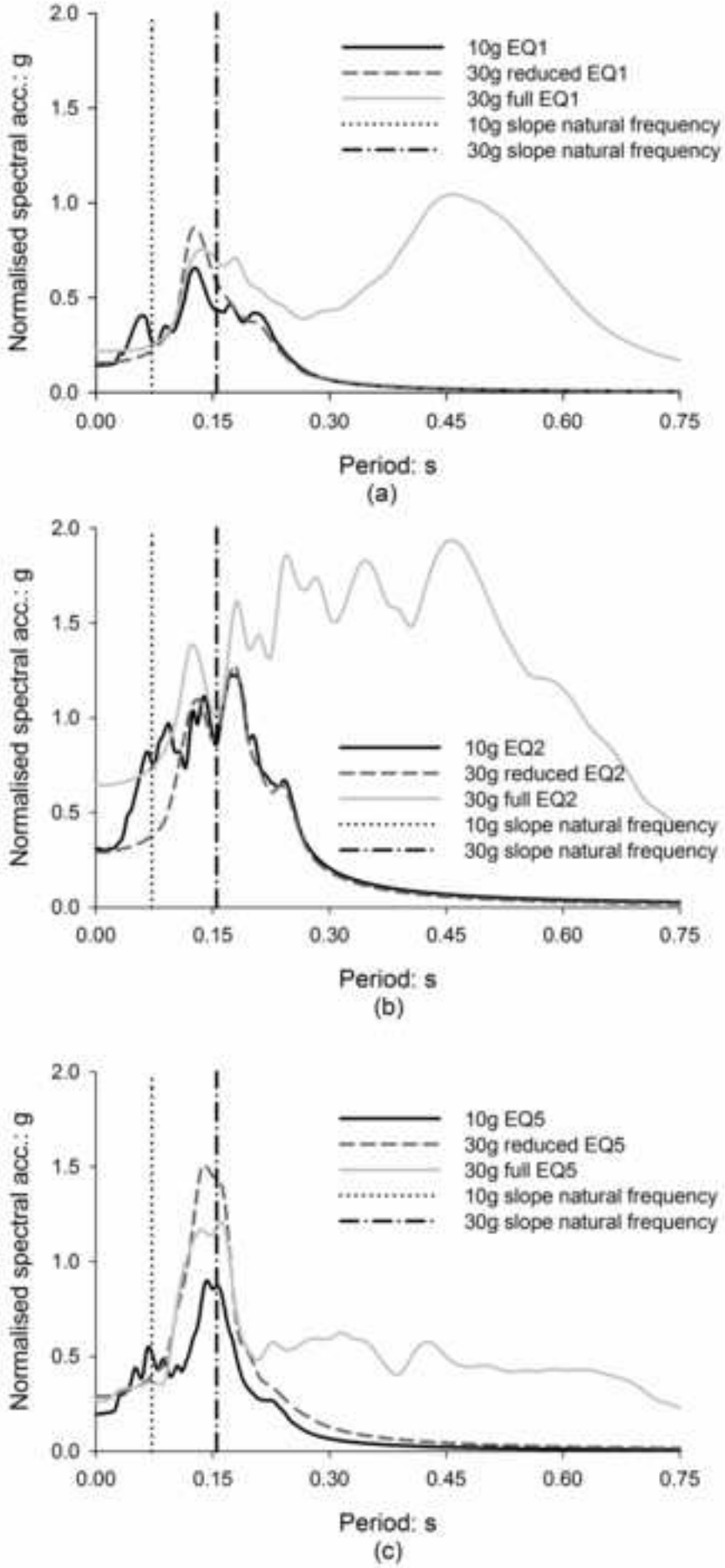

Figure 8

Click here to download Figure Fig8_R1.TIF

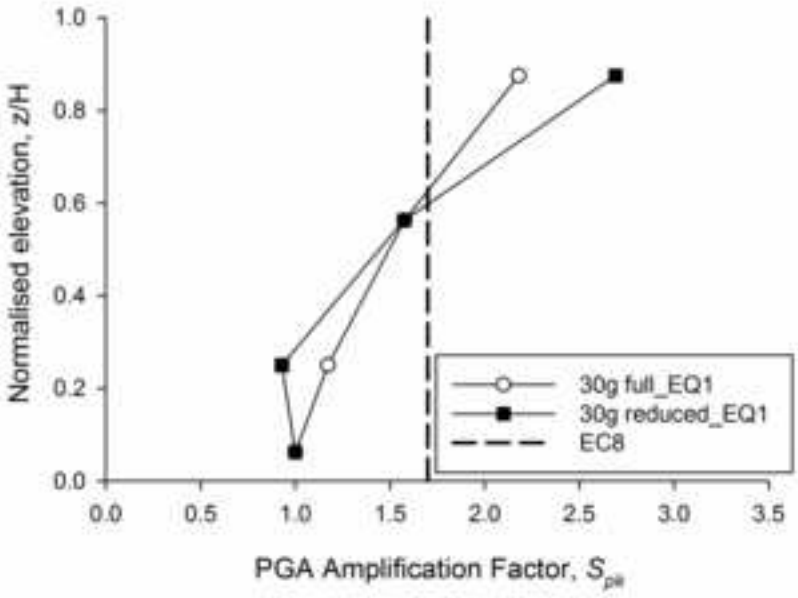

(a)

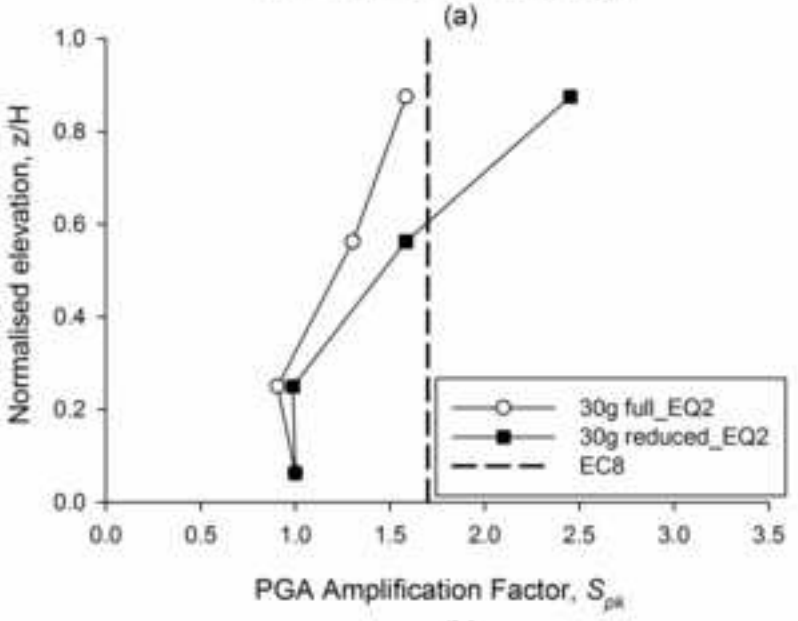

(b)

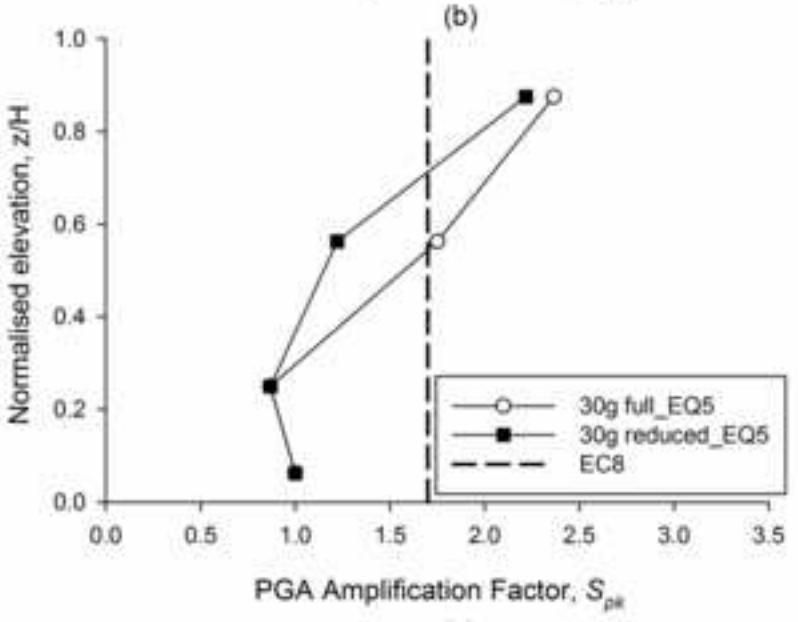

(c)

Figure 9

Click here to download Figure Fig9_R1.TIF

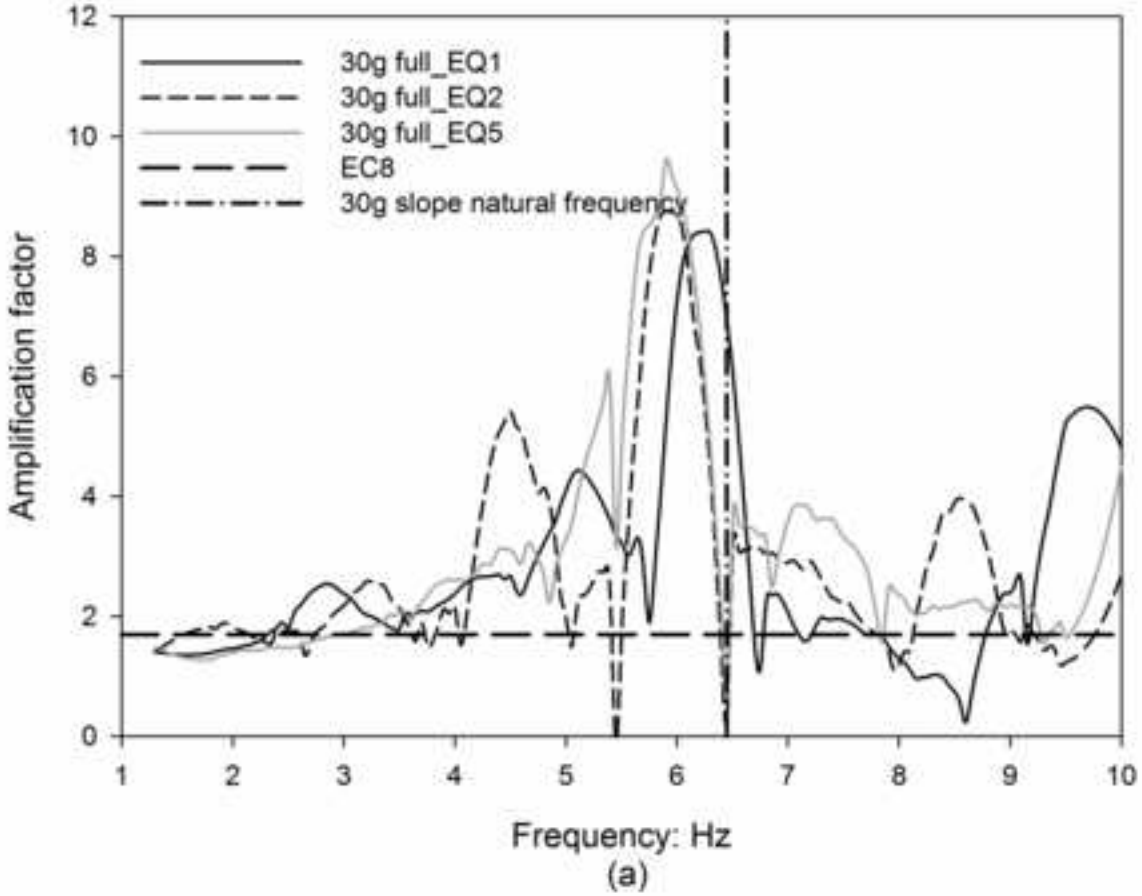

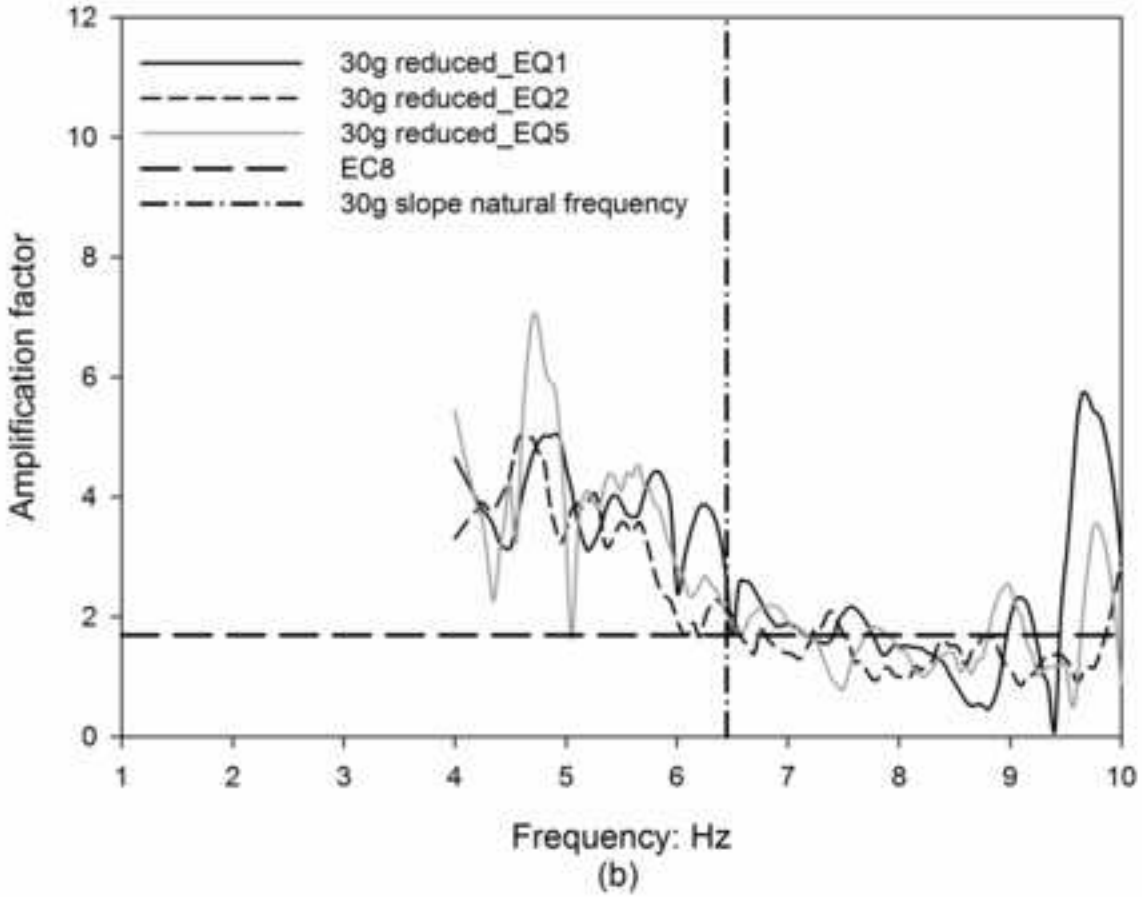

Figure 10

Click here to download Figure Fig10_R1.TIF

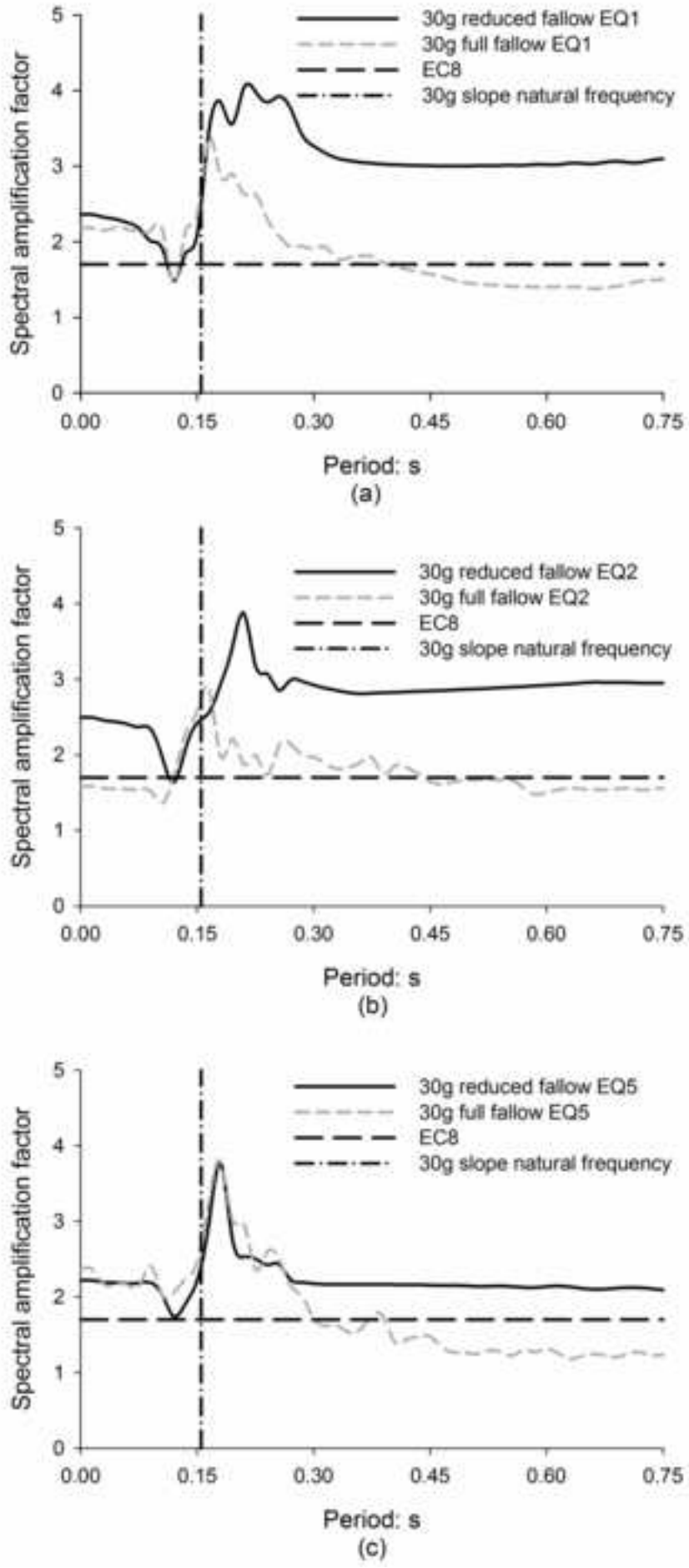

Figure 11

Click here to download Figure Fig11_R1.TIF

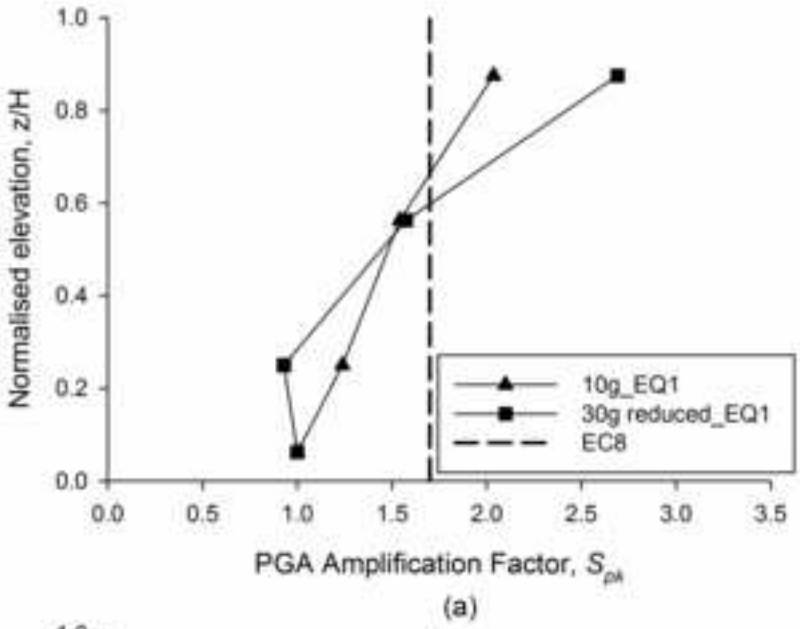

(a)

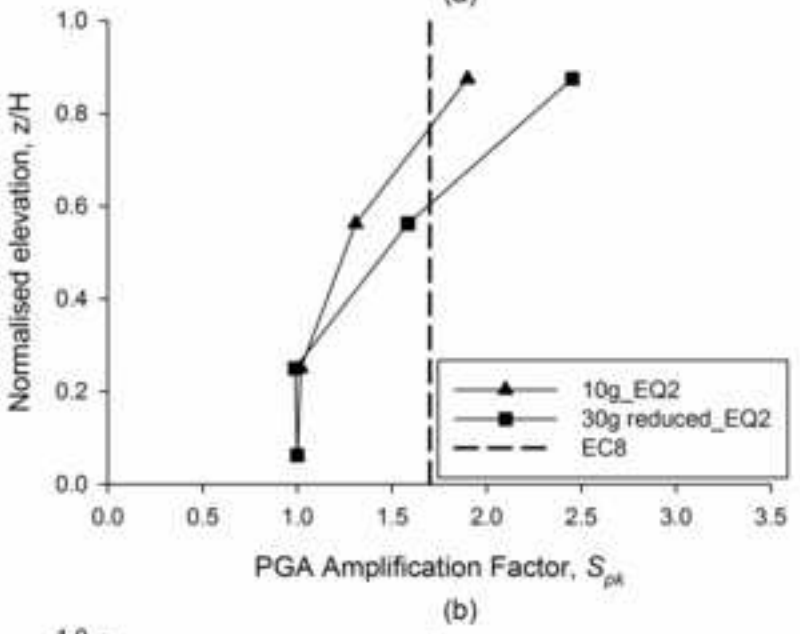

(b)

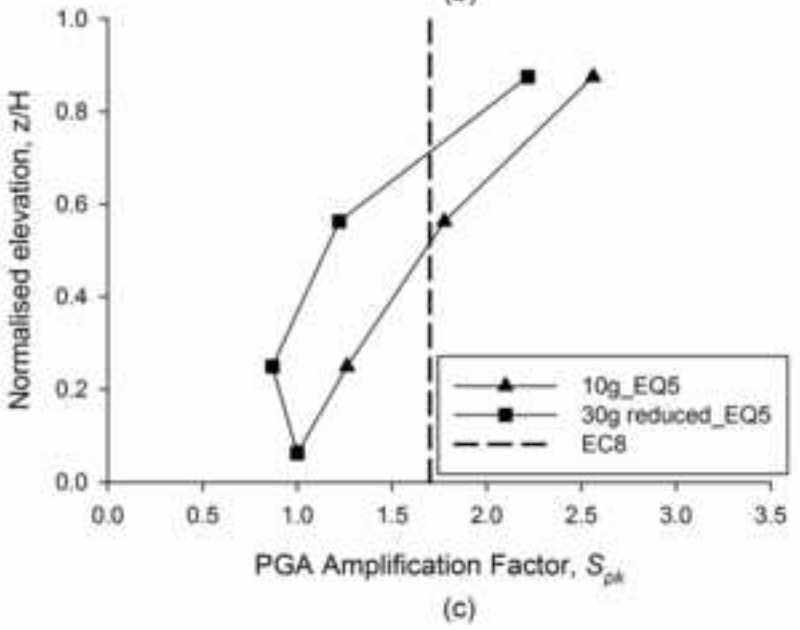

(c)

Figure 12

Click here to download Figure Fig12_R1.TIF

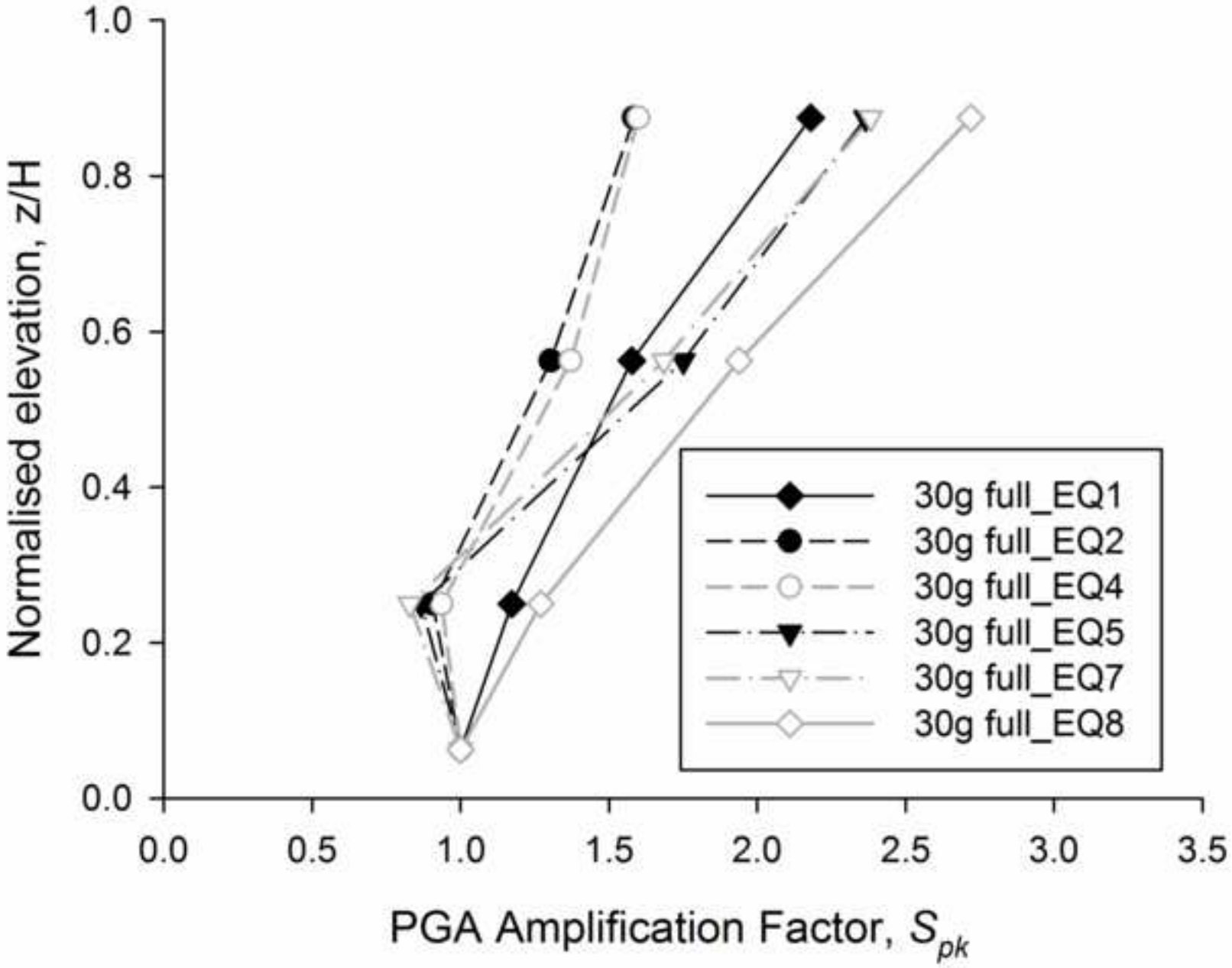

Figure 13

Click here to download Figure Fig13_R1.TIF

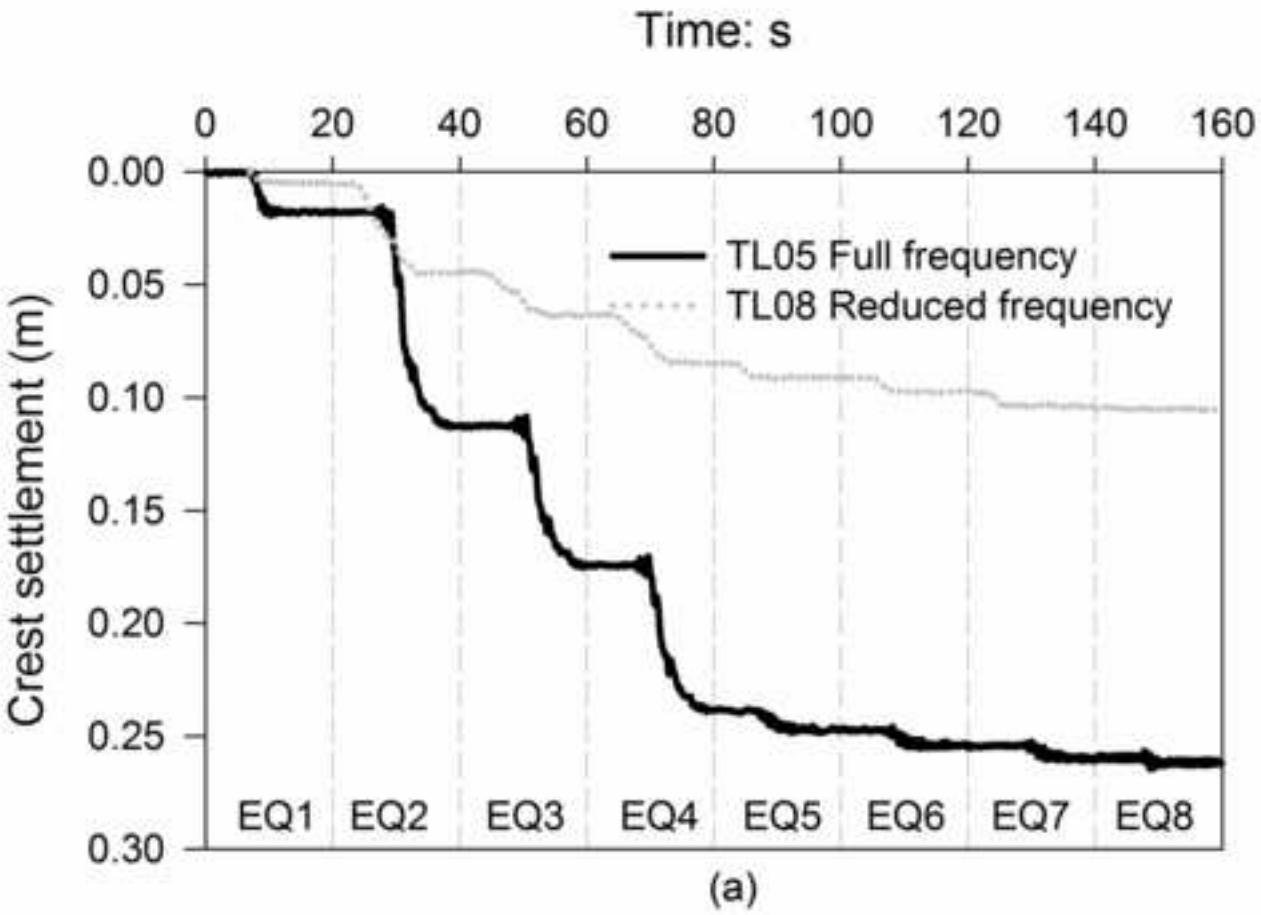

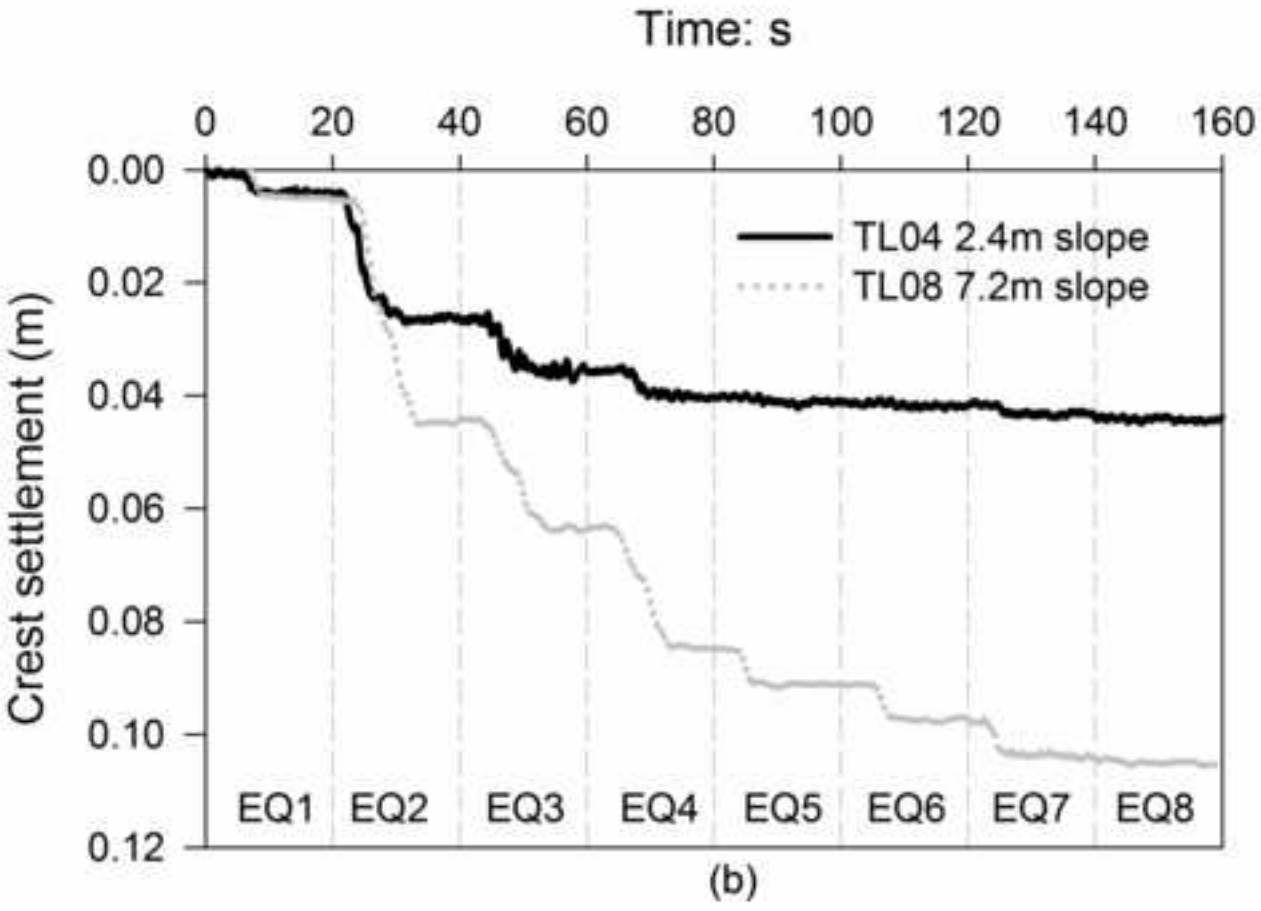

Figure 14

Click here to download Figure Fig14_R1.TIF

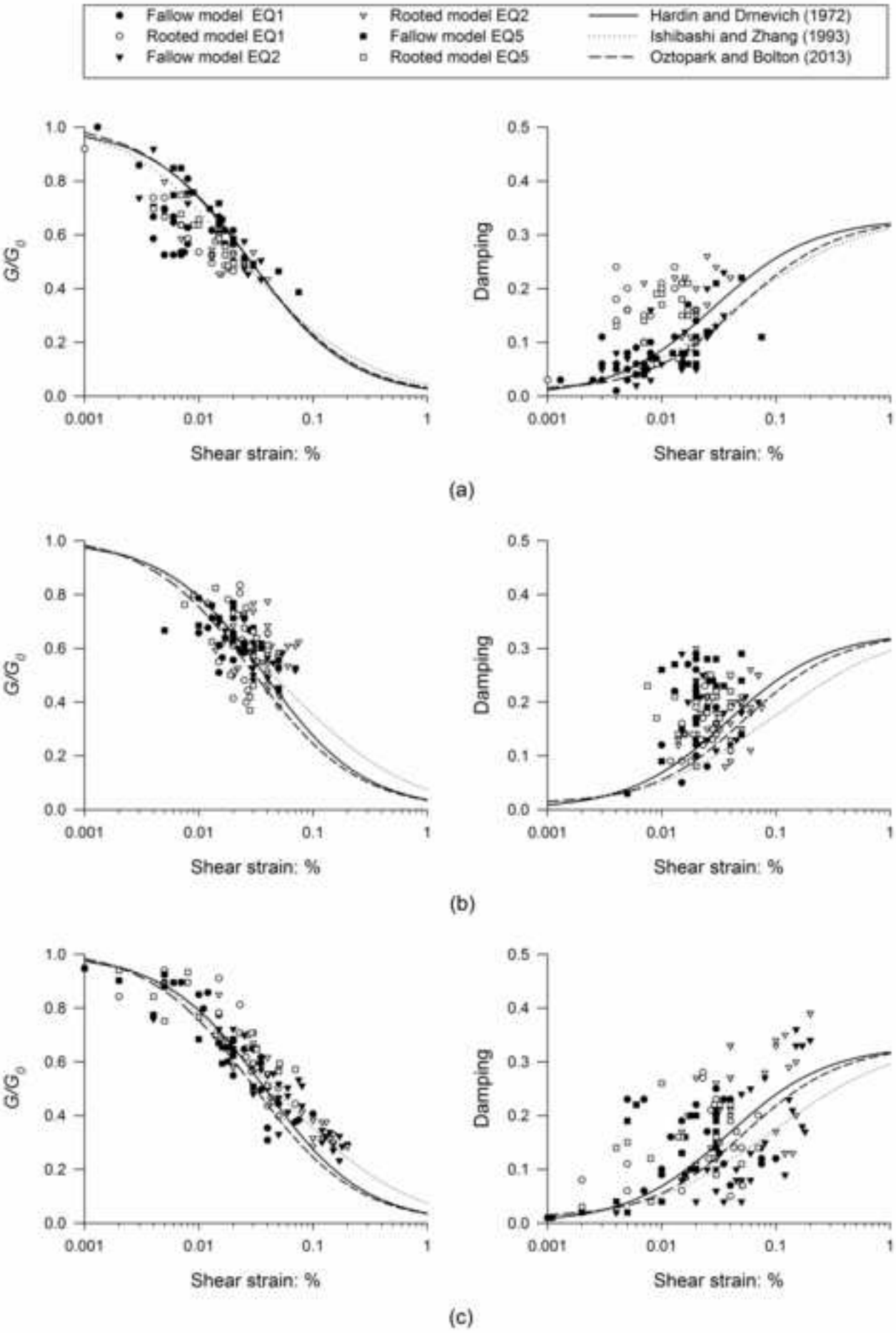

Figure 15

Click here to download Figure Fig15_R1.TIF

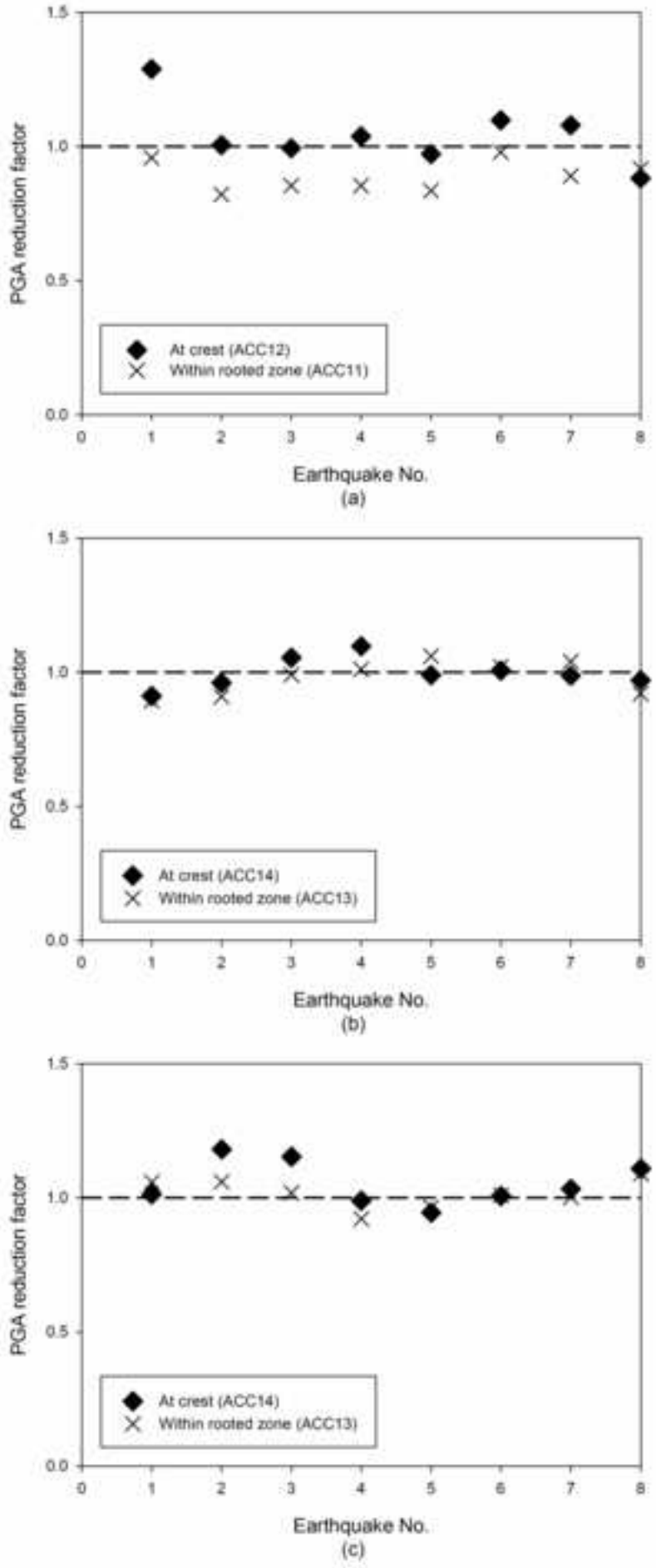

Figure 16

Click here to download Figure Fig16_R1.TIF

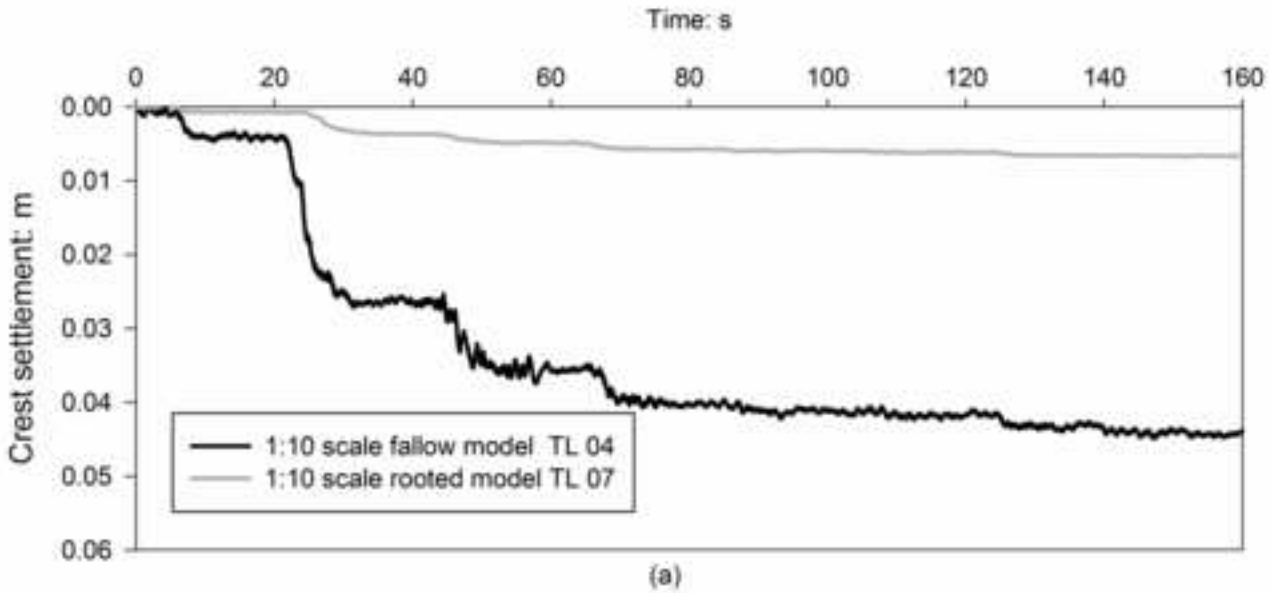

(a)

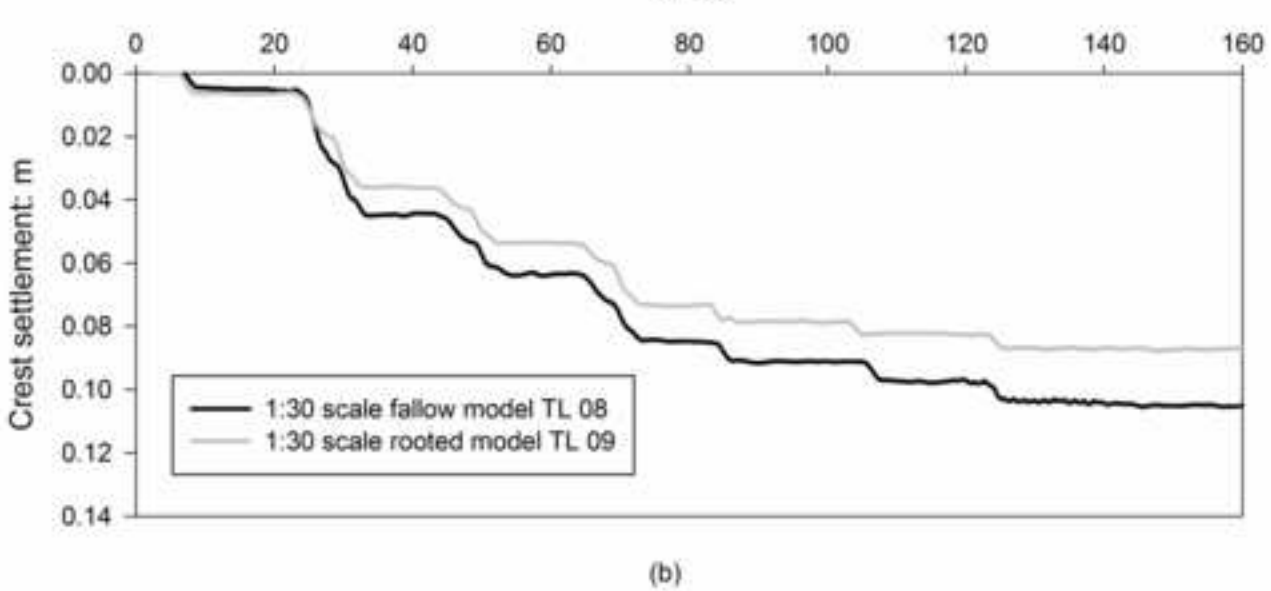

(b)

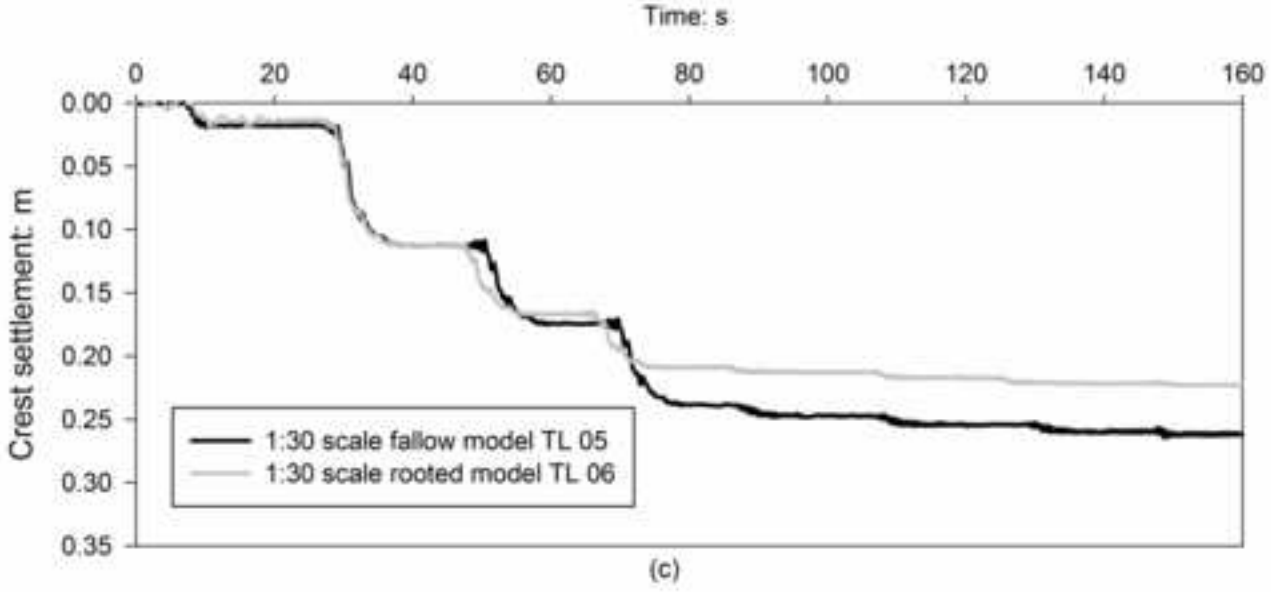

(c)